AD_____

GRANT NUMBER DAMD17-94-J-4120

TITLE: Ret Receptor: Functional Consequences of Oncogenic Rearrangements

PRINCIPAL INVESTIGATOR: Susan S. Taylor, Ph.D.

CONTRACTING ORGANIZATION: University of California, San Diego
La Jolla, California 92093-0934

REPORT DATE: October 1998

TYPE OF REPORT: Final

PREPARED FOR: Commander
U.S. Army Medical Research and Materiel Command
Fort Detrick, Frederick, Maryland 21702-5012

REPORT DOCUMENTATION PAGE

Form Approved
OMB No. 0704-0188

1. AGENCY USE ONLY *(Leave blank)*	2. REPORT DATE	3. REPORT TYPE AND DATES COVERED
	October 1998	Final (15 Sep 94 - 14 Sep 98)

4. TITLE AND SUBTITLE
Ret Receptor: Functional Consequences of Oncogenic Rearrangements

5. FUNDING NUMBERS
DAMD17-94-J-4120

6. AUTHOR(S)
Susan S. Taylor, Ph.D.

7. PERFORMING ORGANIZATION NAME(S) AND ADDRESS(ES)
University of California, San Diego
La Jolla, California 92093-0934

8. PERFORMING ORGANIZATION REPORT NUMBER

9. SPONSORING/MONITORING AGENCY NAME(S) AND ADDRESS(ES)
Commander
U.S. Army Medical Research and Materiel Command
Fort Detrick, Frederick, Maryland 2170-25012

10. SPONSORING/MONITORING AGENCY REPORT NUMBER

11. SUPPLEMENTARY NOTES

12a. DISTRIBUTION / AVAILABILITY STATEMENT
Approved for public release; distribution unlimited

12b. DISTRIBUTION CODE

13. ABSTRACT *(Maximum 200*

The *ret/ptc2* gene was cloned from human papillary thyroid carcinomas, and is the product of a reciprocal chromosomal rearrangement, translocation event between the cAMP dependent protein kinase regulatory subunit Iα (RIα) and the tyrosine kinase domain of the Ret receptor. Ret/ptc2 is a dimer which is autophosphorylated, soluble, and constitutively active. We generated a computer model of the Ret/ptc2 kinase domain, expressed and purified Ret/ptc2, developed a kinase assay to test a variety of peptide substrates and a microinjection assay to compare the structure function relationship of Ret/ptc2 mutants. A number of tyrosine residues within the Ret/ptc2 kinase domain as well as the RIα dimerization domain are critical for eliciting a mitogenic response. A two-hybrid screen identified a number of soluble proteins such as Grb10, PLCγ, and Enigma which are involved in the Ret/ptc2 signaling pathway. Expression of Ret/ptc2 in HEK293 cells have enabled us to link the contributions of the proteins identified earlier to construct a comprehensive model for Ret/ptc2 signaling. The activation of focal adhesion kinase by the Ret/ptc2 oncogene provides a biochemical basis for promoting cell motility which is the fundamental step for metastases of carcinomas.

14. SUBJECT TERMS	15. NUMBER OF PAGES
Breast Cancer, Ret/ptc, receptor tyrosine kinase, structure/ function, signal transduction, metastases, carcinoma	44
	16. PRICE CODE

17. SECURITY CLASSIFICATION OF REPORT	18. SECURITY CLASSIFICATION OF THIS PAGE	19. SECURITY CLASSIFICATION OF ABSTRACT	20. LIMITATION OF ABSTRACT
Unclassified	Unclassified	Unclassified	Unlimited

FOREWORD

Opinions, interpretations, conclusions and recommendations are those of the author and are not necessarily endorsed by the U.S. Army.

____ Where copyrighted material is quoted, permission has been obtained to use such material.

____ Where material from documents designated for limited distribution is quoted, permission has been obtained to use the material.

____ Citations of commercial organizations and trade names in this report do not constitute an official Department of Army endorsement or approval of the products or services of these organizations.

____ In conducting research using animals, the investigator(s) adhered to the "Guide for the Care and Use of Laboratory Animals," prepared by the Committee on Care and use of Laboratory Animals of the Institute of Laboratory Resources, national Research Council (NIH Publication No. 86-23, Revised 1985).

____ For the protection of human subjects, the investigator(s) adhered to policies of applicable Federal Law 45 CFR 46.

__✓__ In conducting research utilizing recombinant DNA technology, the investigator(s) adhered to current guidelines promulgated by the National Institutes of Health.

__✓__ In the conduct of research utilizing recombinant DNA, the investigator(s) adhered to the NIH Guidelines for Research Involving Recombinant DNA Molecules.

__✓__ In the conduct of research involving hazardous organisms, the investigator(s) adhered to the CDC-NIH Guide for Biosafety in Microbiological and Biomedical Laboratories.

PI - Signature Date

TABLE OF CONTENTS

		Page
(1)	FRONT COVER	1
(2)	SF 298, REPORT DOCUMENTATION PAGE	2
(3)	FOREWORD	3
(4)	TABLE OF CONTENTS	4
(5)	INTRODUCTION	5
(6)	BODY	23
(7)	CONCLUSIONS	38
(8)	REFERENCES	39
(9)	BIBLIOGRAPHY	44

INTRODUCTION

Protein phosphorylation is probably the most important mechanism for regulation in eukaryotic cells. The tightly regulated enzymes that catalyze the phosphorylation of proteins, the protein kinases, are important components of signaling pathways that regulate normal cellular functions such as the cell cycle, metabolism, differentiation, memory and response to hormones, to name only a few. Over 400 are now known (1) and mutations that generate unregulated or constitutively activated protein kinases are typically oncogenic.

One of the simplest members of the protein kinase family is the cAMP-dependent protein kinase, cAPK (2). Being one of the best understood members of the protein kinase family, cAPK also serves as a template for the others since all of these enzymes have evolved from a common ancestor and contain a conserved catalytic core. cAPK, in the absence of cAMP, contains two types of subunits, a regulatory (R) subunit and a catalytic subunit (C). The R_2C_2 holoenzyme is catalytically inactive. In the presence of cAMP the complex dissociates into an R_2-$(cAMP)_4$ dimer and 2 free and active C-subunits. The crystal structure of the C-subunit, solved in our laboratory, serves as a structural template for the entire family of protein kinases (3). It defines the folding of the polypeptide chain as well as the positions of the invariant residues that mostly cluster around the active site (4).

The objective of this grant is to characterize a novel oncogenic tyrosine kinase, Ret/ptc2, found in human papillary thyroid carcinomas. Specifically, we want to understand the molecular basis for its constitutive activation and the basis for its oncogenic properties. Ret/ptc2 is a rearranged gene product composed of the cAMP-dependent protein kinase (cAPK) regulatory subunit Iα (RIα) at its N-terminus fused to the tyrosine kinase core of a receptor tyrosine kinase, the Ret receptor (RetR).

Ret Receptor

RetR was cloned from a THP-1 human monocytic leukemia cDNA library, and is expressed in a number of human neuroblastoma and leukemia cell lines as 140-190 kDa glycoproteins (5). Sequence analysis identified it to be a member of the receptor tyrosine kinases, and *in situ* hybridization and mutations of the RetR gene show RetR function is important for enteric neurogenesis and kidney organogenesis in the mouse (6-8) and for normal development of motor and dopaminergic neurons (9). Activation of RetR requires the binding of glial-derived neurotrophic factor (GDNF) to a glycosylphosphatidylinosital linked receptor, GDNFα, and the association of this trimeric complex to RetR (9-12). Homozygous knockout experiments of the GDNF gene result in both kidney agenesis and

the absence of enteric innervation to the digestive system (13). Chromosomal rearrangements of human RetR with other genes and point mutations of RetR have been linked to a number of human cancers and Hirshsprung's disease.

The Ret Oncogene Family

The family of Ret oncogenes can be divided into three separate classes. The first class was produced *in vitro* by transfecting NIH3T3 cells with high molecular weight DNA from human cell lymphomas (14) human colon carcinoma (15) and human stomach cancer tissue (16). The high propensity of the RetR gene to rearrange with other genes is reflected in its name for rearranged upon transfection (14).

The second class consists of missense mutations and truncated forms of RetR that are proposed to result in either hyper- or hypoactivity. These are associated with three dominantly inherited human cancer syndromes: MEN 2A (17), MEN 2B, familial medullary thyroid carcinoma (FMTC) (17,18), and Hirschsprung's disease (19,20).

The third class of Ret oncogenes, isolated from human papillary thyroid carcinomas (PTC) (21-24) consists of 3 subtypes: *ret/ptc1*, *ret/ptc2* and *ret/ptc3*. The 5' end of the each oncogene is a portion of an unrelated gene fused in frame to the identical splice site of the RetR gene resulting in an intact and functional Ret tyrosine kinase.

The PTC-type oncogenes each encode 2 protein isoforms as a result of alternative splicing at the 3' end, and unlike RetR, are completely cytosolic, phosphorylated on tyrosine residues, and constitutively active (23). The 5' end of *ret/ptc1* is a fragment of a new gene designated, H4(DS10S170) (22,25) and the 5' end of *ret/ptc3* encodes a gene designated *ele1* or ret-fused gene, whose gene product does not show sequence identity to known proteins (23,26,27). Unlike *ret/ptc1* and *ret/ptc3*, the N-terminal sequence of *ret/ptc2* (23) encodes approximately 60% of a biochemically well characterized protein, the RIα subunit of cAPK. A comparison of RetR, Ret/ptc2 , and the cAPK RIα-subunit is illustrated in Figure 1.

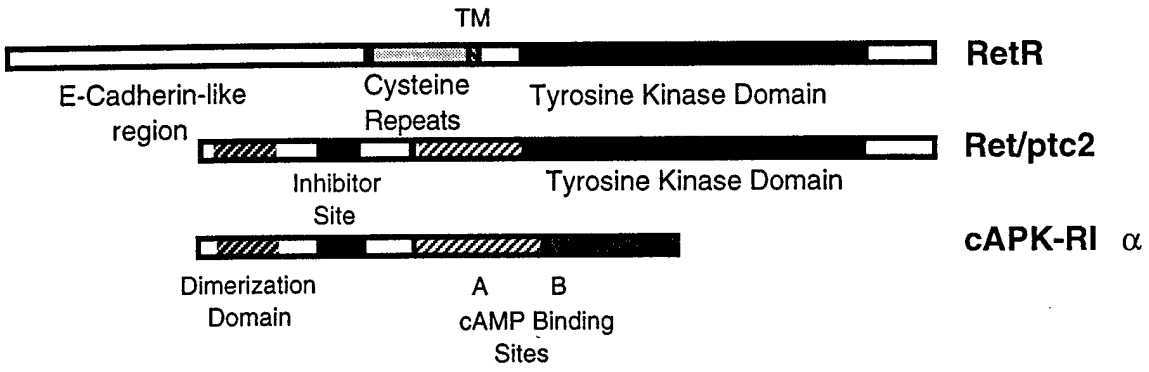

Figure 1. Comparison of RetR, Ret/ptc2, and the cAPK RIα subunit

Regulatory Subunit of cAPK

The regulatory subunit of cAPK maintains the C-subunit in an inactive state by forming a stable R_2C_2 tetramer. A pseudo-substrate inhibition sequence in the R-subunit mimics peptide substrates and fills the peptide binding site of the C-subunit. The binding of cAMP to the R-subunit causes the complex to dissociate and release two active C-subunits.

Although there are several unique gene products in the R-subunit family, all share a well-defined domain structure. The RIα subunit begins with a dimerization domain close to its amino terminus followed by a pseudo-substrate inhibitory region and ends with two tandem cAMP binding domains, A and B. The RIα dimerization domain is stabilized by two antiparallel interchain disulfide bonds (28). Circular dichroism studies of the proteolytically isolated RIα dimerization domain indicate it is predominantly α-helical, and extremely stable to thermal denaturation (29). The crystal structure of a deletion mutant of bovine RIα was solved in our laboratory (30). The splice site of the RIα fragment in Ret/ptc2 is at the beginning of the αC-A helix, thus deleting the last 21% of the A-site cAMP-binding domain and the entire B-site cAMP binding domain.

SPECIFIC AIMS

Our overall long-term goals are to understand the molecular basis for the constitutive activation of Ret/ptc2 and to characterize the physiological function of both Ret/ptc2 and RetR. Our specific aims are the following:

1. To model the kinase core of Ret/ptc2 based on the crystal structures of both the C-subunit of cAPK and the kinase domain of the insulin receptor.

2. To understand the structural features of Ret/ptc2 that are required for its oncogenic properties. To achieve this we have developed an *in vivo* assay to measure the mitogenic response of Ret/ptc2 by nuclear microinjection of *ret/ptc2* into mouse 10T1/2 fibroblasts.

3. To identify Ret/ptc2 associated proteins using a yeast two-hybrid screen.

4. To characterize the biochemical properties of Ret/ptc2 by overexpressing the protein in *E. coli* and human kidney 293 cells. Phosphorylation sites will be mapped and kinetic properties characterized.

5. To construct homologs of Ret/ptc2 using the tyrosine kinase domains of the EGF receptor and the insulin receptor.

We have made excellent progress in each of these areas during the past four years. In this final report, previous results which are detailed in prior annual reports will be briefly summarized.

SUMMARY OF PREVIOUS RESULTS

Microinjection Assay

At the start of the Ret project we constructed a computer model of the RetR kinase core based on the crystal coordinates of both the cAPK C-subunit and the inactive kinase domain of the insulin receptor.

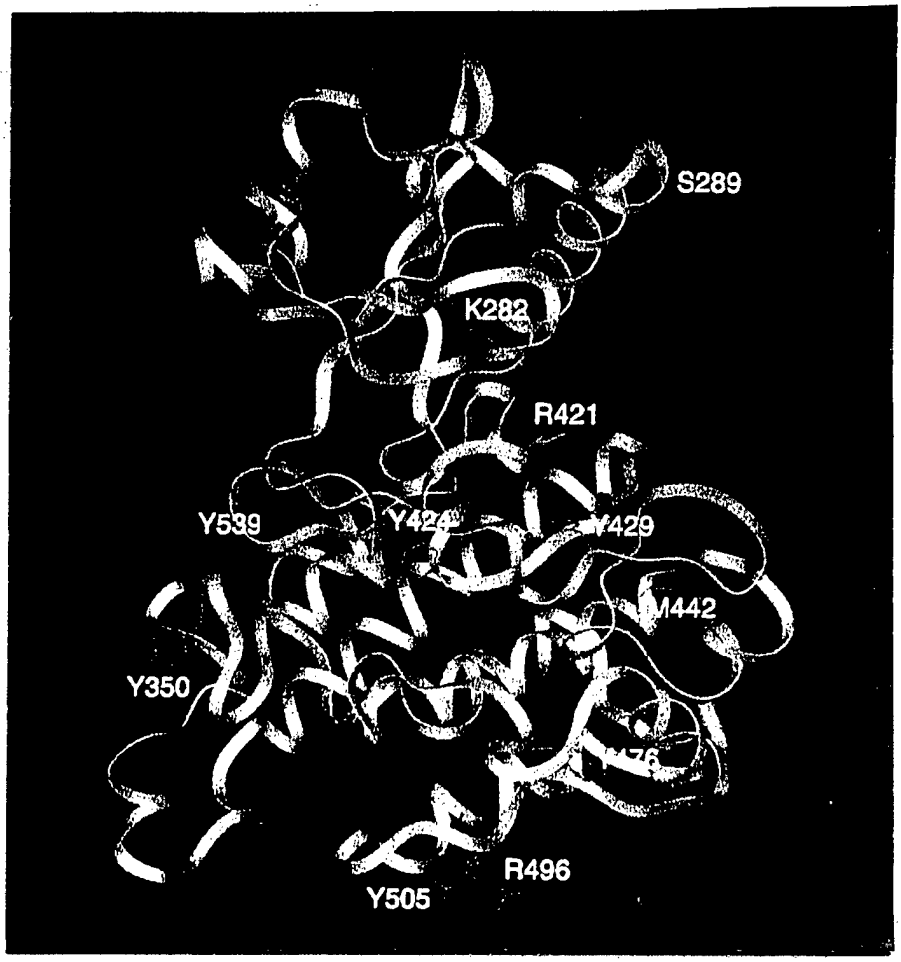

Figure 2. Computer model of the Ret/ptc2 tyrosine kinase domain from residues 237-542. The identified tyrosine residues have been shown to be important in eliciting a mitogenic response in the microinjection assay. This model does not include tyrosine 586 which is located at the C-terminus. Highlighted residues correspond to point mutants analyzed in Figure 3.

We developed a nuclear microinjection assay of *ret/ptc2* and mutants thereof into mouse 10 T1/2 fibroblasts to quantitate DNA synthesis by 5-bromodeoxyuridine (BrdU) incorporation (31). These studies confirmed the point mutations at S289P, R421Q and R496G identified in Hirschsprung's disease inactivates Ret/ptc2. The MEN2B mutation at M442T did not abolish the mitogenic response of Ret/ptc2 as expected. Microinjection of epiderrmal growth factor receptor (EGFR) homolog, RIα/EGFR, consisting of the entire EGFR cytoplasmic domain, showed this chimera was as mitogenically active as Ret/ptc2. Truncation of the EGFR C-termnal tail which contains tyrosine residues necessary for recruiting Src homology (SH2) domains of downstream signaling effectors abolished the mitogenic response. The physiological consequences of C-terminal truncations of the wild-type EGFR however, result in unaltered catalytic and signaling efficiency. The

microinjection assay identified several key tyrosine residues in the kinase domain of Ret/ptc2 at positions 505 and 586 which are presumably necessary for signal transduction. These results are illustrated in Figure 3 and the mutated residues are shown in Figure 2.

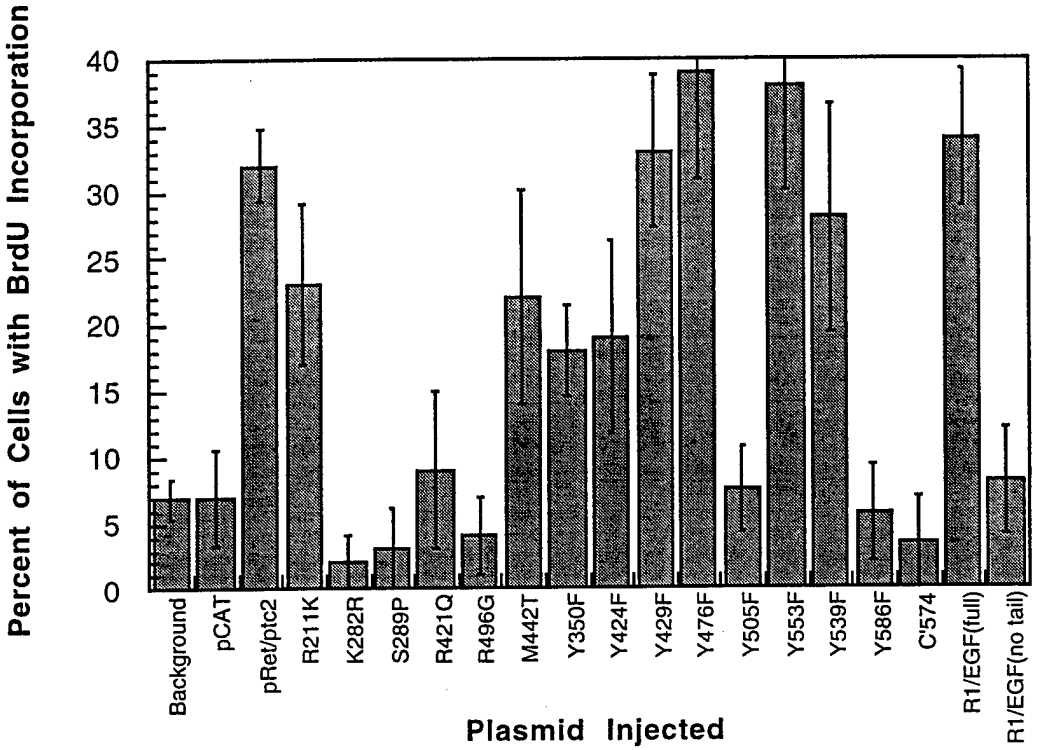

Figure 3. Mitogenic response of various constructs in the microinjection assay. pCAT is a chloramphenicol transferase reporter that was microinjected as a negative control.

The microinjection assay identified the dimerization domain within the Ret/ptc2 RIα sequence to be critical for eliciting a mitogenic response in 10 T1/2 fibroblasts. Analysis of RIα deletion mutants of Ret/ptcc2 are summarized in Figure 4.

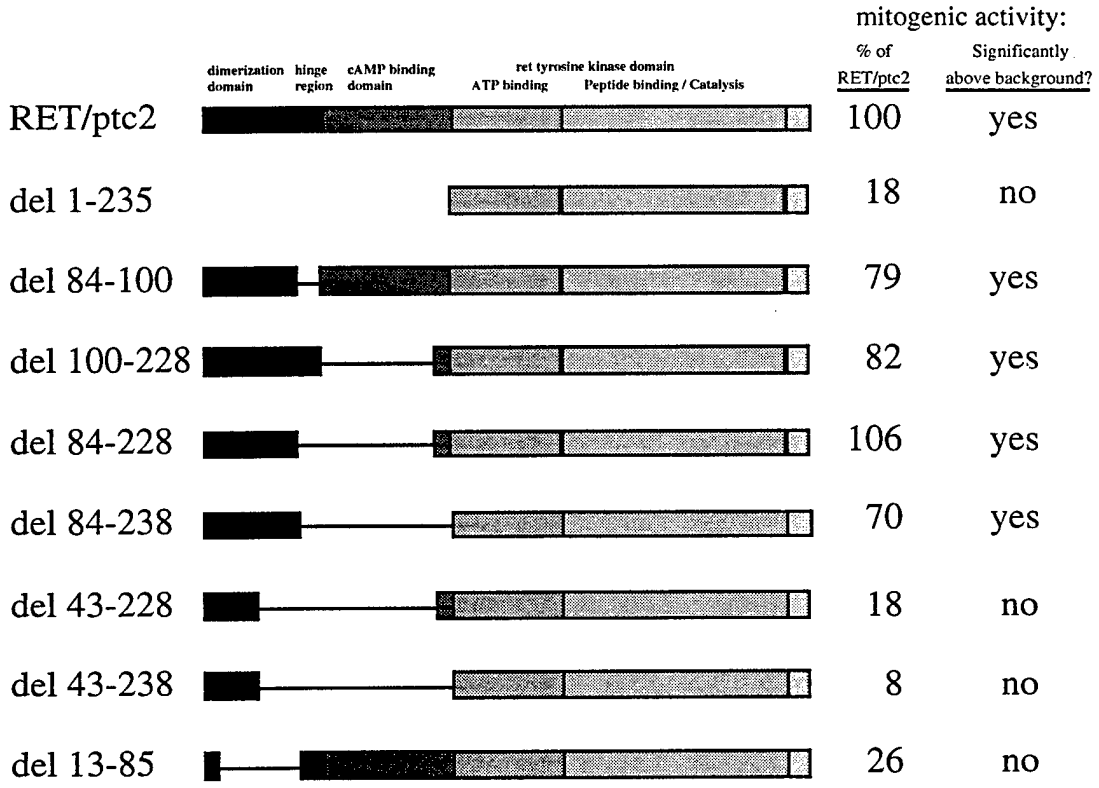

Figure 4. Mitogenic response of various Ret/ptc2 deletion constructs in the microinjection assay.

Ret/ptc2 Associates with PLCγ, Grb10, and the Enigma LIM2/3 Domains

Using the kinase domain of Ret/ptc2 as the bait, we screened a murine embryonic library using a yeast two-hybrid system (32). We identified the SH2 domains of Grb10 and phospholipase C γ (PLCγ) associates with residues Y429 and Y539 of Ret/ptc2, respectively, which corroborated earlier reports (33,34). In addition, we found the C-terminal LIM2/3 domains of Enigma (35) interact with Ret/ptc2 at residue Y586 (36). Further refinement identified the Enigma LIM2 domain associates with a kinase inactive Ret/ptc2 mutant, Ret/ptcY282R, whereas neither the SH2 domains of Grb10 or PLCγ interact with Ret/ptc2Y282R. These results indicate the Enigma LIM2 interaction is independent of autophosphorylation at residue Y586. Full-length Enigma binds to both Ret/ptc2 and the Ret/ptc2 kinase domain but not to a Ret/ptc2 mutant lacking Y586, C574, (37). The interactions between Ret/ptc2 and the SH2 domains of Grb10 and PLCγ and the Enigma LIM2/3 domains were quantitated using a β-galactosidase assay (Figure 5).

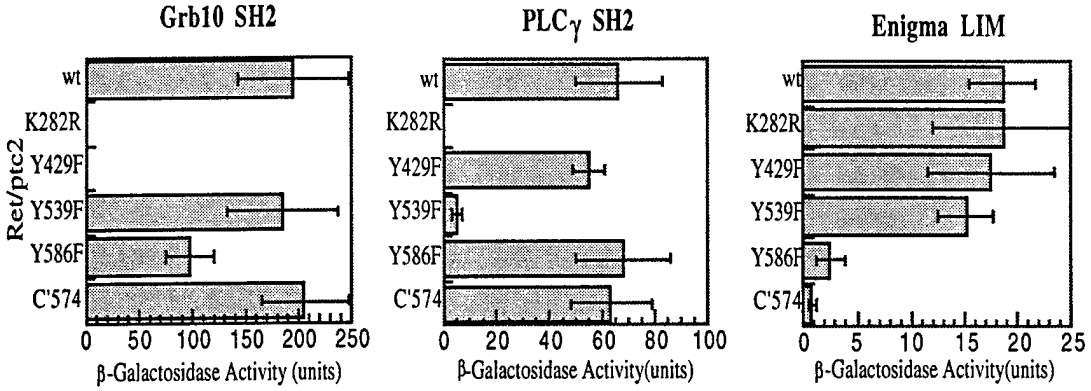

Figure 5. β-galactosidase activity of yeast co-transfected with constructs expressing Ret/ptc2 as bait (wild-type or tyrosine to phenylalanine mutants) and with Grb10-SH2, PLCγ-SH2, or Enigma-LIM2/3 as prey.

Co-injection of *ret/ptc2* and the three C-terminal LIM domains of Enigma, *C275,* into mouse 10T 1/2 cells reduced the mitogenic response of Ret/ptc2 whereas co-injection with full-length *enigma* or the N-terminal portion of Enigma, *N279*, did not alter the mitogenic response (36). The Enigma LIM2 domain was found to specifically interact with Ret/ptc2; LIM domains from zyxin failed to interact with Ret/ptc2. Co-injection of *C275* or full-length Enigma, *FL*, with *RIα/EGFR* did not inhibit the induction of DNA synthesis. These results are summarized in Figure 6.

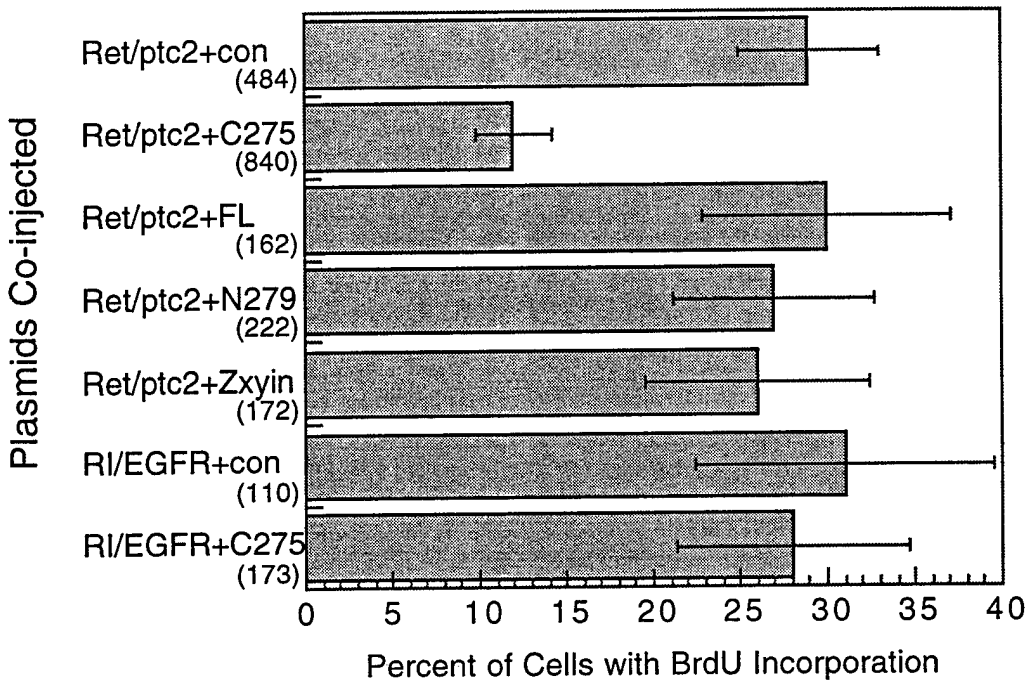

Figure 6. Mitogenic response of Ret/ptc2 co-injected with the control expression plasmid (con), full-length Enigma (FL), C-terminal half of Enigma (C275), or N-terminal half of Enigma (N279).

Enigma and Ret/ptc2 Co-Distribute in Micro-Injected Mouse 10 T1/2 Cells

The distribution of Ret/ptc2 concentrates about the cell periphery, including regions resembling focal adhesions and the actin cytoskeleton (38). Full-length Enigma displayed a distribution pattern similar to that of Ret/ptc2, with pronounced staining of the cell edges and some cytoskeletal components. A deletion mutant of Enigma lacking the N-terminal PDZ domain exhibited a diffuse, cytoplasmic staining pattern, while a mutant lacking all three C-terminal LIM domains retained the wild-type distribution (Figure 7).

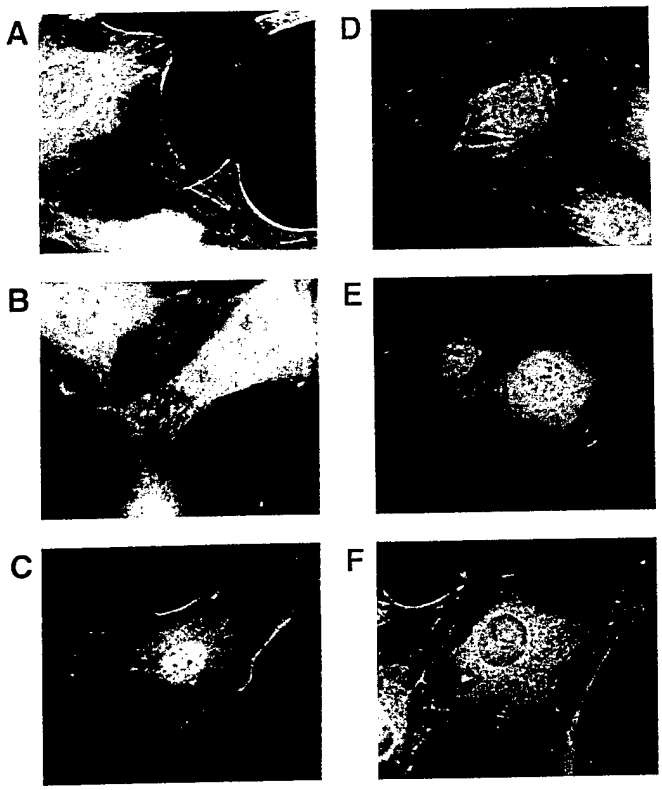

Figure 7. A- C: Sequence requirements for the sub-cellular targeting of Ret/ptc2. Fibroblasts microinjected with various Ret/ptc2 expression plasmids were fixed four hours after injection and immunofluorescently stained using Ret antibodies. Constructs injected coded for: (A) wild-type Ret/ptc2, (B) Ret/ptc2-C'574, a mutant where the last 22 amino acid residues are deleted, including the Enigma binding site, and (C) Ret/ptc2-Δ13-84, a dimerization domain deletion mutant. D-F: Sequence requirements for the sub-cellular targeting of Enigma. Cells injected with constructs expressing HA-tagged forms of Enigma were stained for immunofluorescence with anti-HA-tag monoclonal antibodies. Plasmids expressed the following HA-tagged protein: (D) full-length Enigma, (E) the C-terminal 275 residues of Enigma, which contain the three LIM domains, (F) the N-terminal 279 residues of Enigma, which contain the PDZ domain.

Further characterization of Enigma binding to Ret/ptc by confocal microscopy of microinjected mouse 10 T1/2 cells show the two proteins co-distribute (Figure 8).

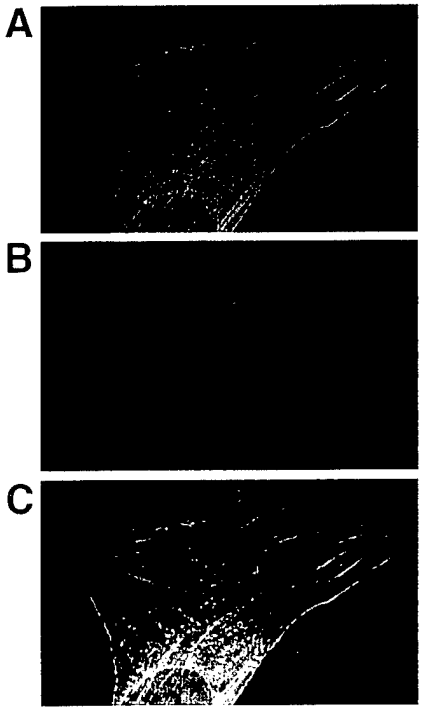

Figure 8. Mouse 10T1/2 fibroblasts co-injected with expression plasmids of Ret/ptc2 and HA-tagged Enigma were fixed four hours after injection, subjected to immunofluorescent staining, and then imaged by confocal microscopy. (A) Enigma distribution shown by fluorescein linked to anti-HA-tag monoclonal antibody. (B) Ret/ptc2 distribution shown by fluorescence of Cy-5 linked to anti-Ret antibody, (C) digital overlay of the two fluorescent signals.

Model for Enigma and Shc Binding to Ret/ptc2

Since the Ret/pt2 Enigma binding site was reported by a number of groups to bind to the phosphotyrosine binding (PTB) site of the adaptor protein Shc (39,40), we wanted to investigate whether Y586 is capable of binding to both proteins. Using a yeast two-hybrid approach, we found Shc binds to Ret/ptc2 in a phosphorylation dependent fashion. The catalytically inactive Ret/ptc mutant, Ret/ptc2Y282R, failed to interact with Shc PTB domain as well as Ret/ptc2Y586F and the C-terminal truncation mutant, C'574. The Shc SH2 domain did not interact with Ret/ptc2.

To elucidate the roles of Shc and Enigma binding to Ret/ptc2 we engineered a chimeric form of Ret/ptc2 that would bind Shc and not Enigma and another chimera that would bind Enigma and not Shc. To test the importance of Enigma anchoring of Ret/ptc2, the "unanchored" C-terminal deletion form of Ret/ptc2, C'574, was fused to the N-terminal 279 residues of Enigma to make a chimeric protein referred to as C'574-PDZ. To engineer a form of Shc that would bind to Ret/ptc2 in the absence of tyrosine 586, PLCγShc was constructed in which the PTB domain of Shc was replaced with the N-terminal SH2

domain of PLCγ (Figure 9A). This SH2 domain of PLCγ interacts with Y539 of Ret/ptc2 (36,41).

These chimeric proteins were first tested in the two-hybrid system and then further characterized in transient transfections. Wild-type Shc interacted with Ret/ptc2, but failed to interact with any of the Ret/ptc2 forms lacking tyrosine 586, including the chimeric C'574-PDZ (Figure 9B, left panel). The PLCγShc chimeric adapter protein bound to all forms of Ret/ptc2 except the unphosphorylated, kinase-inactive K282R mutant (Figure 9B, right panel).

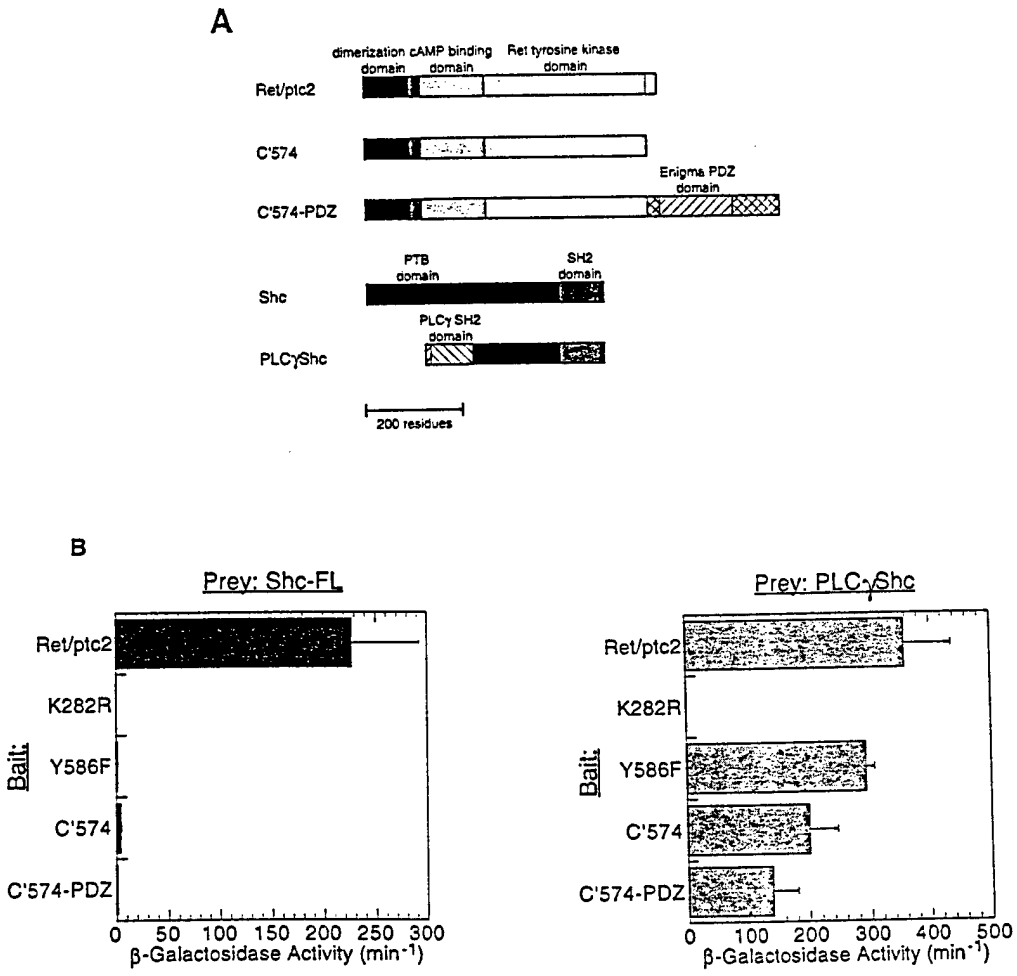

Figure 9. Characterization of interactions between Ret/ptc2 and Shc or PLCγ-Shc. The yeast two-hybrid system was used to monitor the interactions between various Ret/ptc2-LexA constructs aand either Shc-VP16 or PLCγ-Shc-VP16 fusions. (A) Schematic representation of the fusion proteins constructed. B) β-galactosidase activity of yeast co-transformed with the Ret/ptc2 and Shc constructs. Results shown are averages of units of activity from four solution assays, with error bars representing the standard deviations.

This pattern of interaction was confirmed in co-transfected human embryonic kidney 293 cells. Co-expression of Ret/ptc2 with Shc resulted in Shc tyrosine phosphorylation, while Ret/ptc2 constructs incapable of binding to Shc were also unable to phosphorylate Shc (Figure 10). In contrast, C'574 and C'574-PDZ were both able to phosphorylate PLCγShc.

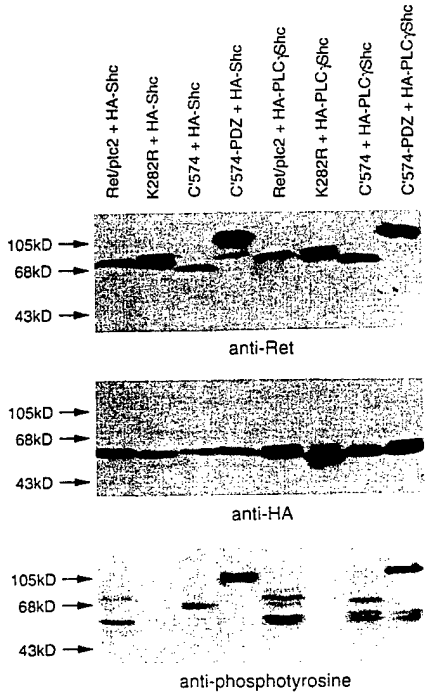

Figure 10. Phosphorylation of Shc and PLCγ-Shc by Ret/ptc2 constructs. Kidney 293 cells were cotransfected with plasmids expressing a form of Ret/ptc2 and either HA-tagged Shc (HA-Shc) or PLCγ-Shc (HA-PLCγShc). The Ret/ptc2 constructs expressed wild-type Ret/ptc2, a kinase-inactive point mutant (K282R), a C-terminal truncation mutant (C'574), or a C-terminal replacement with the PDZ domain of Enigma (C'574-PDZ). Twenty-four hours after transfection, the cells were harvested, and lysates were separated by SDS-PAGE. Proteins were then transferred to PVDF membranes and detected with either anti-Ret (upper panel), anti-HA (middle panel), or anti-phosphotyrosine (lower panel) antibodies.

To test which of the interactions are required for Ret/ptc2 mitogenic signaling, the chimeric proteins were evaluated in the mitogenic microinjection assay. As shown previously (36), the C'574 mutant of Ret/ptc2, which does not bind to Enigma and Shc, was not mitogenically active (Figure 11). Adding the Enigma PDZ domain to make C'574-PDZ failed to increase mitogenic activity, despite the fact that this chimeric protein was sub-cellularly localized in the same distribution as that of Enigma and wild-type Ret/ptc2 (data not shown). PLCγShc did not exhibit any mitogenic activity in this assay, and its interaction with C'574 was not sufficient to rescue the mitogenic activity of this non-

localized form of Ret/ptc2. Only co-expression of PLCγShc with C'574-PDZ resulted in significant stimulation of mitogenic activity (Figure 11).

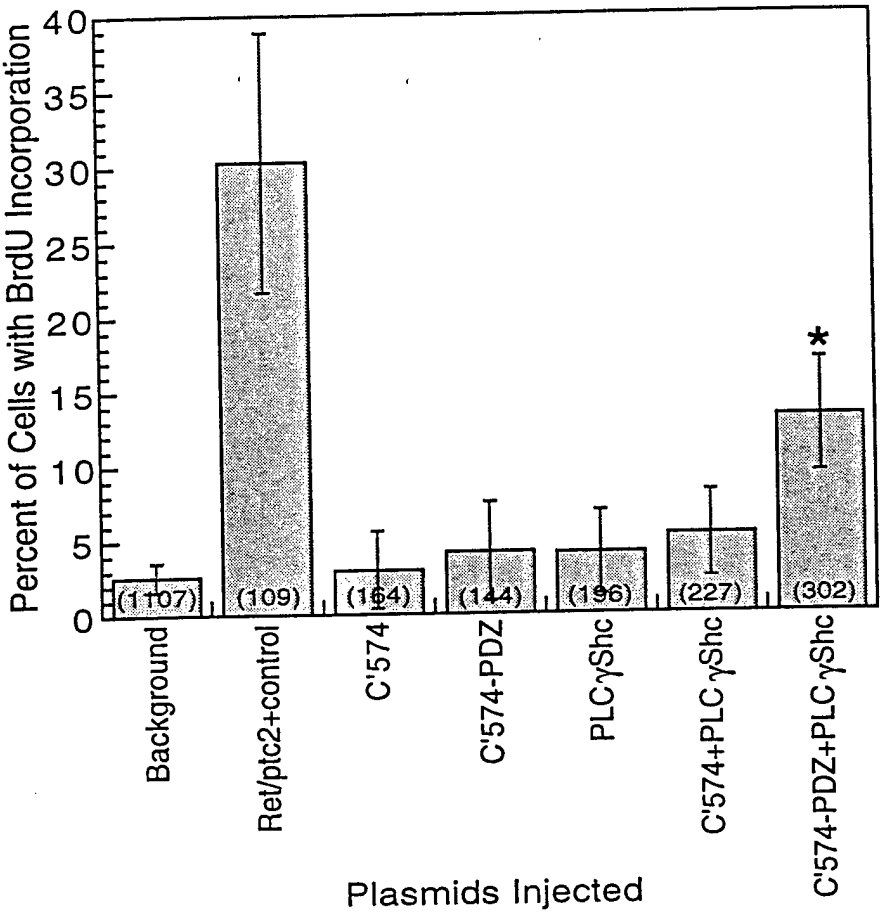

Figure 11. Mitogenic activity of Ret/ptc2 constructs coexpressed with PLCγ-Shc. In each case, constructs were injected at 100 μg/ml, while background represents uninjected cells. Cells were then assessed for entry into S-phase by immunofluorescent detection BrdU incorporation. The fraction of injected cells positive for BrdU incorporation is shown with error bars displaying the 95% confidence interval calculated using the standard error of proportion. The numbers in parentheses are the total number of injected cells. The asterisk (*) denotes cells co-injected with plasmids for C'574-PDZ and PLCγShc were significantly above background in BrdU incorporation ($p < .001$).

To verify that a complex of Ret/ptc2 dimer binding to both Shc and Enigma was formed *in vivo*, affinity precipitation experiments were carried out using lysates from transfected 293 cells. The cells were co-transfected with constructs expressing HA-tagged Shc and either Ret/ptc2, or Ret/ptc2 Δ13-84. Both Ret/ptc2 and the form lacking the dimerization domain, Ret/ptc2 Δ13-84, bound to Enigma GST-LIM2 fusion protein. However, Shc was only precipitated in the presence of dimeric, wild-type Ret/ptc2. This

result demonstrates that a Ret/ptc2 dimer is capable of simultaneously binding to the LIM domain of Enigma and to Shc. From these results, we propose a model for Ret/ptc2 signaling through its dual association with Shc and Enigma (Figure 12).

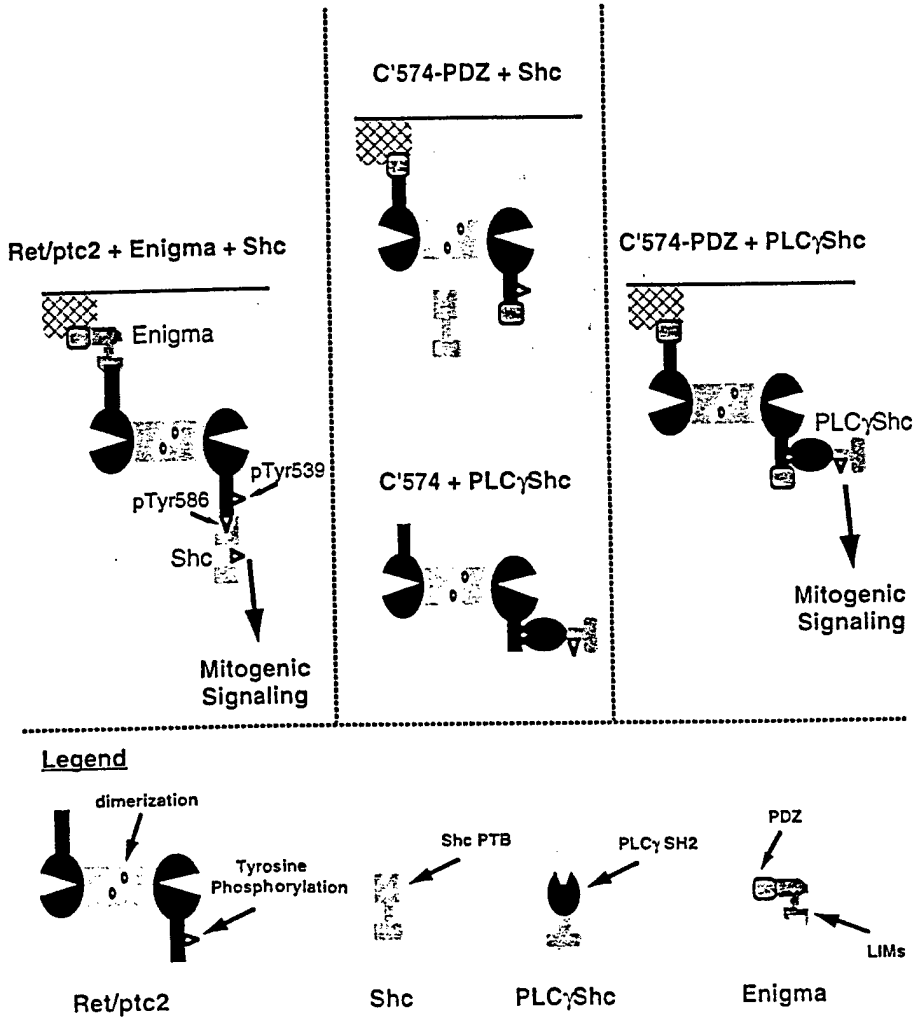

Figure 12. Proposed model for Ret/ptc2 mitogenic signaling. The left panel illustrates functions of Enigma and Shc in Ret/ptc2 signaling. The center panel summarizes results indicating that functions of either Enigma or Shc alone are insufficient for Ret/ptc2 activity. The right panel shows restoration of Ret/ptc2 mitogenic activity by reconstitution of both Enigma and Shc functions via chimeric molecules.

Screening Ret/ptc2 Peptide Substrates

Expression of Ret/ptc2 in human embyronic kidney 293 cells (HEK293) provided a source of unpurified protein to screen a number of peptide substrates. The following table summarizes these results.

TABLE I. Peptide Substrate Screen

Peptide Substrate	Sequence	μmoles Pi incorporated min^{-1}
angiotensin II	DRVYHPF	2.1
35b	RRKSRDVY$_{424}$EEDS-NH_2	0.089
36b	RRKSEEMY$_{505}$RLML-NH_2	0.21
37	KRRDY$_{539}$LDLA	1.6
21	KRRDY$_{539}$LDLAASTPSDSL	0.83
39	RKVGPGY$_{350}$LGSG-NH_2	0.01
42	KRRENKLY$_{586}$GRIS-NH_2	0.42
43	KRRSRDVY$_{424}$EEDSY$_{429}$VKRS-NH_2	0.53
44	RPAQAFPVSY$_{687}$SSSG	0
45	KRREEDSY$_{429}$VKRS-NH_2	0.11
49	AEEEEYFELVAKKKK	0.01

Although the angiotensin peptide appears to be a better substrate for Ret/ptc2, peptide 37 is a more specific substrate. Peptide substrate 37 contains Y539 which was found in the yeast two-hybrid screen to associate with PLCγ. Peptide 37 is a shorter version of peptide 21, however the degree of phosphorylation of peptide 37 by Ret/ptc2 is significantly increased 2-fold. Mutation of Y350 to phenylalanine decreased the mitogenic response by 30 % (31), however, peptide 39 was poorly phosphorylated by Ret/ptc2 *in vitro*. Peptide 44 corresponds to the juxtamembrane sequence of RetR (42). Both Y350 and Y687 were identified to be autophosphorylated by 2-dimensional phosphopeptide mapping of immunoprecipitated RetR isolated from transiently transfected COS cells with *proto-ret* and subsequently autophosphorylated *in vitro* with [γ-^{32}P]-ATP (43). Peptides 35b and 45 contain Y424 and Y429, respectively, of Ret/ptc2 which correspond to Y1158 and Y1162 in the insulin receptor (44). Phosphorylation of these residues in the insulin receptor is

critical for activity. Phosphorylation of either tyrosine residue in peptide substrate 35b or 45 is minimal, however, when both residues are present within a single peptide, as in peptide 43, there appears to be a synergistic effect. Peptide 49 represents a consensus peptide substrate sequence for EGFR (45). This peptide substrate is not recognized by Ret/ptc2.

The ATP Km was determined to be 51-61 μM ATP for Ret/ptc2 expressed in 293 cells. The following plot (Figure 13) is a representative example of the kinase assay data. Each point is the average of 3 data points, the standard errors for the data points is 9 % or less, and the correlation factor is 0.997.

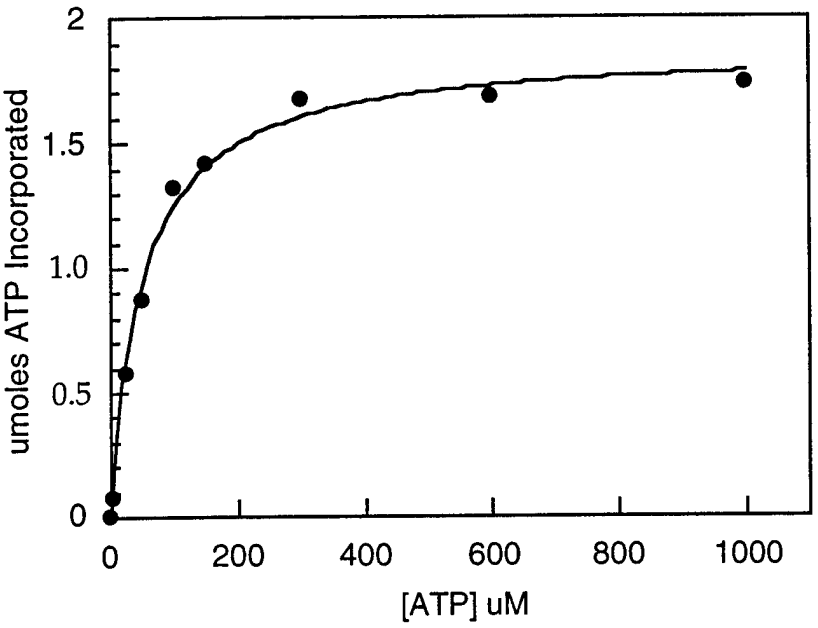

Figure 13. ATP Km for Ret/ptc2 expressed in human kidney 293 cells.

Analysis of the RIα/EGFR and RIα/InsR Chimeric Proteins

In order to investigate the role of the RIα dimerization domain in the activation of the tyrosine kinase domains of RTKs, we constructed chimeric genes of both the epidermal growth factor receptor (EGFR) and the insulin receptor (InsR) to mimic the *ret/ptc2* gene. In the microinjection assay, the EGFR chimera elicited a mitogenic response similar to that of Ret/ptc2, however, removal of the C-terminal tail, residues 959-1186, abrogated this response (31). Similar to Ret/ptc2, the EGFR chimera is autophosphorylated when expressed in 293 cells and the protein can be phosphorylated *in vitro*. The ATP Km was

determined to be 62-79 μM in the kinase assay using the EGFR 1173 peptide substrate at 1 mM. The ATP Km for the EGFR kinase domain is 48-57 μM. These results indicate that the contribution of the RIα subunit to the activity of the EGFR kinase activity is not significant *in vitro*. However, the strong mitogenic response elicited by the EGFR chimera suggests that the *in vivo* contribution of the dimerization domain is significant. We have recent evidence that the RIα subunit dimerization domain interacts with an anchoring protein, D-AKAP1 (46) which serves to localize RIα within the cytosol. In contrast to the EGFR chimera, expression of the InsR chimera in 293 cells resulted in an inactive, unphosphorylated protein. These results suggest that the activation of the Ret/ptc2 and EGFR kinase domains occurs via an intramolecular process whereas the InsR kinase may be activated by an intermolecular event.

Expression and Purification of His_6-Ret/ptc2

Although the expression of Ret/ptc2 in human embryonic kidney 293 cells, Sf9 insect cells, and *E. coli* was successful, the quantity of Ret/ptc2 produced in these expression systems was too low for quantitative purification, and extensive biochemical and biophysical characterization. We attempted the expression of His_6-Ret/ptc2 in the wild-type strain, GS115 of the methylotrophic yeast, *Pichia pastoris*, in collaboration with Jim Hoeffler and Tom Purcell at Invitrogen (Carlsbad, CA). Small-scale expression preparations of either secreted or intracellularly expressed His_6-Ret/ptc2 were analyzed by SDS-PAGE and Western analysis using the Ret antibody. Intracellularly expressed His_6-Ret/ptc2 was overexpressed whereas the secreted protein was not detectable. We found however expressed His_6-Ret/ptc2 in the wild-type *P. pastoris* host strain degraded with time at -80 °C. The degradation of His_6-Ret/ptc2 in unlysed frozen cells was further complicated by co-purification of over-expressed alcohol oxidase using our established protocol of metal chelate affinity chromatography.

The following section of this report will concentrate on the work accomplished in the last year. We have continued to work on the purification of Ret/ptc2 from the methylotrophic yeast, *Pichia pastoris*, and to define how Ret/ptc2 signals in mitogenesis. We present evidence on how Ret/ptc2 can initiate metastases of papillary thyroid carcinomas by interfering with focal adhesion protein signaling pathways.

MATERIALS AND METHODS

Plasmid Constructs

Ret/ptc2 was subcloned into the PmlI-NotI sites of the *Pichia* vector, pPICZb (Invitrogen), containing a thrombin cleavage site at its 3' end, and expressed in the *pep4⁻ his4⁻* host strain SMD1168 (E. Komives, UC San Diego).

Expression in Pichia pastoris Strain SMD1168

Ret/ptc2/pPICZB was linearized with PmeI (New England BioLabs) to transform the *pep4⁻ his4⁻Pichia pastoris* strain SMD1168 cells by electroporation in 0.2 cm cuvettes (Bio-Rad) at 1500V, 25μF and 200ω. Pulsed cells were incubated in 1 M sorbitol at 30 °C without agitation for 1 hour, and plated onto 2% agar YPDS (1% yeast extract, 2% bacterial peptone, 2% dextrose, 1M sorbitol) plates containing 100 mg/l zeocin (Invitrogen) and incubated at 30 °C for 2 days. Colonies were purified by restreaking onto fresh YPDS/zeocin plates. Single colonies were grown overnight at 30 °C and 300 rpm in buffered glycerol complex medium (1% yeast extract, 2% peptone, 100 mM KH_2PO_4, pH 6.0, 1.34% yeast nitrogen base with ammonium sulfate without amino acids, 4 x 10^{-5}% D-biotin, 1% glycerol, BMGY). Cells were pelleted and resuspended in buffered methanol complex medium (BMMY, replacing 1% glycerol in BMGY with 0.5 % methanol) to induce Ret/ptc2-His_6 expression for 48 hours. Cells were pelleted, resuspended in the lysis buffer described above, and lysed 8 times for 30 seconds each at room temperature in a mini-beadbeater (BioSpec Prooducts) with 425-600 μm acid-washed glass beads (Sigma). Proteins in the souble fraction were separated by SDS-PAGE followed by Western analysis to determine Ret/ptc2-His_6 expression. Log-phase uninduced cultures of high expression recombinants were frozen in 20% glycerol and stored at -80 °C. Fermentation of *ret/ptc2* /SMD1168 recombinants was accomplished in a basal salts medium containing PTM salts (47) with the following exceptions: the pH of the culture was maintained at 5.3,the medium was supplemented with 0.4% L-histidine every 24 hours at 25-40 ml/l, expression of Ret/ptc2-His_6 was induced for 4 days by growth in 100 % methanol, cells were harvested by centrifugation, and the cell pellet was stored at -80 °C.

Purification of Ret/ptc2-His_6

Eleven grams of frozen cells were thawed and rinsed briefly in the following lysis buffer: 20 mM Tris-Cl, pH 8, 100 mM NaCl, 10 % glycerol, 5 mM EDTA, 5 mM β-ME, 50 μg/ml TLCK, 100 μg/ml TPCK, 1 μg/ml leupeptin, 0.1 mM PMSF, 0.1 mM 1, 10-o-phenanthroline, 0.1 mM amino benzene ethyl sulfonyl fluoride (ABESF). Cells were pelleted by centrifugation at 3000 x g for 10 minutes at 4 °C, resuspended in 30 mls lysis

buffer, and lysed 10 times for 30 seconds each in an MSK cell homogenizer (B. Braun Biotech Inc.) with 16 gms of 425-600 μm acid-washed glass beads, and cooling the sample 2-3 minute in an ice water bath between lysing. Lysates were centrifuged at 31000 x g for 12 minutes at 4 °C, and the supernatant fraction, S1, was withdrawn and precipitated with 55% NH_4SO_4 at 4 °C for 30 minutes. Precipitated proteins were removed by centrifuging the sample at 31000 x g for 10 minutes at 4 °C, and the supernatant fraction, S2, was dialyzed (Spectra/Por 12-14,000 MW cutoff) extensively into the lysis buffer described above. Proteins in the dialysate were bound to 20 mg DE-52 resin at 4 °C and eluted with a linear NaCl gradient (100-300 mM). Peak Ret/ptc2-His_6 fractions were determined by SDS-PAGE and Western analysis, extensively dialyzed against 20 mM Tris-Cl, pH 8, 100 mM NaCl, 5 mM EDTA, 5 mM β-ME, 10 % glycerol, 5 mM EDTA, 0.1 mM ABESF and filtered through a 0.8 μm/0.2 μm Acrodisc PF syringe filter (Gelman). Ret/ptc2-His_6 was purified by a second anion exchange chromatography by binding onto an Uno Q6 column (Bio-Rad) and eluting with a linear salt gradient using a BioLogic Workstation (Bio-Rad) at 4 °C. Peak fractions were determined by SDS-PAGE and Western analysis as described above, concentrated in a stirred cell concentrator (Amicon) at 4 °C, and purified to homogeneity by preparative gel filtration using the BioLogic Workstation fitted with a Pharmacia Superdex 200 preparative gel filtration column in 50 mM HEPES, pH 8, 200 mM NaCl, 5 mM β-mercaptoethanol and 10 % glycerol at 4 °C.

Mammalian Cell Culture

HEK293 and NIH3T3 cells were a generous gift from the laboratory of G.N.Gill (UC San Diego) and maintained at 37 °C, 8% CO_2. HEK293 cells were grown in Dulbecco's Modification of Eagle's Medium (DMEM) containing 1 gm/l glucose with L-glutamine, 5% fetal bovine serum (FBS) , 5% enriched calf serum (ECS) and 1% fungibact . NIH3T3 cells were grown in DMEM containing 4.5 gm/l glucose with L-glutamine, 10% ECS and 1% fungibact.

Plasmids and Site-Directed Mutagenesis

ret/ptc2 was a generous gift from M. A. Pierotti (Istituto Nazionale Tumori, Milan, Italy). *p2FTL* and β-galactosidase/CMV were a generous gift from the laboratory of G. N. Gill (UC San Diego). Murine *p125^{FAK}Y397F-(HA)3* was a generous gift from D. D. Schlaepfer (Scripps Research Institute). *ret/ptc2Y586F* was constructed using the QuikChange kit (Stratagene) using the manufacturer's protocol.

Transfection of HEK293 Cells

Plasmid DNA was amplified in the *E. coli* strains, DH5α or XLI-Blue (Stratagene), and purified using the Qiagen endotoxin-free maxi plasmid kit according to the maufacturer's protocol. NIH3T3 and HEK293 cells were transfected using either the calcium phosphate method (48), or the Qiagen Effectene Transfection Kit using the manufacturer's protocol. Cells were harvested 36-48 hours post-transfection in the existing medium, rinsed 2x with phosphate buffered saline (PBS) and homogenized with a nylon microfuge tube pestle on ice in 100 µl of the following lysis buffer: 50 mM HEPES, pH 8, 150 mM NaCl, 10 % glycerol, 5 mM β-mercaptoethanol, 1 µg/ml leupeptin, 100 µg/ml TPCK, 50 µg/ml TLCK, 0.01 mM 1,10-o-phenanthroline, 0.1 mM PMSF, 1 mM Na_3VO_4, 0.1 mM AEBSF. Cell lysates were cleared by centrifugation at 14,000 x g at 4 °C for 10 minutes and the supernatant fraction (S1) was withdrawn for immunopreciptation, kinase assays, or discontinuous sodium dodecylsulfate polyacrylamide gel electrophoresis (SDS-PAGE) (49).

Antibodies and Western Immunoanalysis

The peptide antigen sequence corresponding to residues 535-551 of Ret/ptc2 was synthesized in the laboratory E. Komives (UC San Diego) on a Milligen 9050 PepSyn peptide synthesizer using standard Fmoc methodology with the pentafluorophenyl esters of the amino acids and either hydroxybenzotriazole or more lately hydroxyasabenzotriazole as the activator. The peptide antigen was desalted by reverse-phase HPLC, and conjugated to keyhole limpet haemocyanin (Calbiochem) with glutaraldehyde (50). Polyclonal antibodies were isolated from rabbit serum (Cocalico Biologicals, Reamstown, PA), purifed from CM Affi gel Blue Gel (BioRad), precipitated with 45% ammonium sulfate, and eluted from protein A conjugated agarose (Pierce). Proteins separated by SDS-PAGE (10% T, 4.5% C) were transferred to 0.45 µm PVDF membranes (Millipore or Bio-Rad) in 10 mM CAPS, pH 11, 10% methanol for 1 hour at 4 °C and 100V. Blots were rinsed briefly in 0.5 M Tris-Cl, 1.5 M NaCl, 1% Tween 20, (TTBS) and incubated in either 5% nonfat milk/TTBS (α-Ret or α-PY-20 antibodies) or 2% bovine serum albumin (BSA)/TTBS (α-paxillin antibodies) overnight. Blocked blots were incubated in the following primary antibodies: **PY-20**: monoclonal mouse phosphotyrosine antibodies (Transduction Labs) at 1:2000 in 5% nonfat milk/TTBS, **paxillin**: monoclonal mouse paxillin antibodies (Transduction Labs) at 1:1000 in 1% BSA/TTBS, **HA**: monclonal 12CA5 mouse antibody (laboratory of H. Bourne, UC San Francisco) at 1:5000 in 1% BSA, **c-*Myc***: polyclonal mouse c-*Myc* antibody (Santa Cruz or Invitrogen) at 1:2000, **Ret**: polyclonal rabbit Ret antibodies at 1:200000 in TTBS. Blots were rinsed and then incubated in either anti-mouse

horseradish peroxidase (HRP) at 1:2000 (Amersham/USB), anti-rabbit HRP (Amersham/USB) at 1:2000 or anti-rabbit alkaline phosphatase (Boehringer Mannheim) and visualized by chemiluminescence (Pierce) or developed with nitro blue tetrazolium and 5-bromo-4-chloro-3-indolyl phosphate according to the manufacturer's protocol (Promega).

Immunoprecipitation

Four micrograms of polyclonal rabbit $p125^{FAK}$ antibodies (Upstate Biotechnology), 8-10 µg affinity purified polyclonal rabbit Ret antibody, or 3 µg 12CA5 antibodies were added to isolated S1 fractions from HEK293 cell lysates and incubated up to 2 hours at 4 °C on a rotating wheel. Agarose beads conjugated with protein A (Pierce) were equilibrated in fresh lysis buffer and 30-35 µl of the slurry was added to each S1 fraction and incubation was continued for 45 minutes or overnight. Samples were centrifuged to pellet the resin and the resin was washed 4 x with 300 µl each of fresh lysis buffer. 45-90 µl of 1x laemmli loading dye was added to the resin for SDS-PAGE. All other fractions were diluted 1:1 with 2x laemmli loading dye.

Expression of GST-Pax_{LIM4} Protein

The four C-terminal LIM domains (residues 318-561) of avian paxillin (51) was expressed as a GST-fusion protein, GST-Pax_{LIM4}, in the vector, pGEX-2TK (Pharmacia), in the *E. coli* strain, BL21(DE3) (Novagen). Expression was induced with 1 mM isopropylthio-β-galactoside for 2 hours at 37 °C. Harvested cells were lysed by sonication in 20 mM Tris-HCl, pH 7.5, 100 mM NaCl, 5 mM benzamidine-HCl, 1% Triton X-100, 10 µg/ml leupeptin, 10 µg/ml aprotinin, and the lysate cleared by centrifugation. Fusion proteins were purified on glutathione agarose (Sigma) and the washed beads were resuspended in the buffer described above to a final concentration of 0.1 mg/ml GST-Pax_{LIM4}.

Kinase Assay of GST-Pax_{LIM4}

Ten micrograms of GST-Pax_{LIM4} agarose beads were incubated with 10 µl S1 fraction isolated from HEK293 cells transfected with either TE, pH 8 or *ret/ptc2* for 10 minutes at room temperature (RT). Reactions were stopped by centrifuging the samples at RT for 5 minutes to pellet the resin, and the resin rinsed 2x with 50 µl ice-cold lysis buffer. 10 µl of 1x laemmli loading dye was added to the rinsed resin, samples heated at 100 °C for 3 minutes and separated by SDS-PAGE. The destained polyacrylamide gel was dried between 2 sheets of cellophane in 10% ethanol, 5% glycerol and exposed to Kodak XAR film at -80 °C with intensifying screens.

Kinase Assay of HA-JNK and c-Myc-ERK2

The methods used were similar to that reported previously (52). Briefly, 1 µg HA antibody or c-*Myc* antibody was added with 10 µl 10% protein A-sepharose to each S1 fraction isolated from co-transfected HEK293 cells containing identical concentrations of total protein to immunoprecipitate overnight at 4 °C. Beads were washed 3x with 500 µl each of 50 mM Tris-Cl, pH 7.5, 150 mM NaCl, 0.5% Tween-20 (TTBS), once with kinase assay buffer: 25 mM HEPES, pH 7.4, 20 mm $MgCl_2$, 0.1 mM Na_3VO_4, 1 mM PMSF, 10 µg/ml leupeptin, 20 mM β-gycerol phosphate, 2 mM dithiothreitol, and the final pellet was resuspended in 20 µl kinase assay buffer. 2.8 µg GST-c-Jun or 5 µg myelin basic protein and 1 µl [γ-^{32}P]-ATP was added and the reactions incubated at 30 °C for 20 minutes. Reactions were quenched by the addition of 6x laemmli loading dye and the proteins were separated by SDS-PAGE. Dried gels were exposed to film at -80 °C with intensifying screens.

Luciferase Assay

Transfected HEK293 cells were harvested in the existing medium, rinsed twice with PBS, resuspended in 100-300 µl 100 mM KPO_4, pH 7.8, 1 mM DTT, and lysed by freeze/thaw 3x in dry ice/isopropanol and 37 °C. Lysates were cleared by centrifugation and samples were incubated on ice until assayed. Three microliters of each S1 fraction was added to 300 µl 100 mM KPO4, pH 7.8, 5 mM ATP, 15 mM $MgSO_4$ and the reaction was initiated with 100 µl 1 mM luciferin (Analytical Luminescence Laboratory). Luminescence was measured in a Monolight 2001 luminometer for 10 seconds at RT. Each sample was assayed for transfection efficiency by incubating an aliquot of each S1 fraction in 500 µl 50 mM Tris-Cl, pH 7.5, 100 mM NaCl, 10 mM $MgCl_2$, 0.75 mM o-nitrophenyl β-D galactopyranoside 6-phosphate (Sigma), until a visible color was detected. Reactions were quenched with 500 µl 1M Na_2CO_3 and quantitated at OD_{420}. Duplicate luminescence values from triplicate transfections were corrected for transfection efficiency by dividing each value by volume corrected OD_{420} readings per transfection, and averaging the final values. Standard errors were calculated using the standard error of the average which was typically 6% or less. The vector average value was set to 1.0 and average values for each sample was divided by the vector average value and presented as a fold-activation above or below 1.0.

Microinjection of NIH3T3 Cells and Immunostaining

NIH3T3 cells were plated at 1.67 x 10^4 onto sterile 12 mm (Fisher) glass cover slips in 60 mm plastic culture dishes and incubated overnight at 37 °C, 10% CO_2. Prior to injection, each cover slip was transferred into a separate 35 mm culture dish containing fresh DMEM + 10% FBS. Endotoxin-free plasmid DNA was diluted to 100 µg/ml in 40 mM NaCl, 50 mM HEPES, pH 7.6, and loaded into a glass injection needle (Kopf). Cells were nuclearly injected with the injection needle mounted on an automatic micromanipulator (Eppendorf). Microinjected cells were incubated at 37 °C, 5% CO_2 and fixed 5 hours post-injection with 3.7% formaldehyde in PBS for 5 minutes at RT, rinsed briefly in PBS and permeabilized 0.3% Triton X-100/PBS. Cells were immunostained following an established protocol (31). Cover slips were mounted onto glass slides (Fisher) with gelvatol.

RESULTS

I. Ret/ptc2 Expression and Purification

In the *Pichia pastoris* expression system Ret/ptc2 was expressed as a fusion protein containing a thrombin cleavage site at the end of the Ret/ptc2 primary sequence, followed by a C-*Myc* epitope, and a His_6 tag at its C-terminus. The predicted size and isoelectric point of the full-length protein is 71358 kDa and 6.21, respectively. Western analysis of a Ret/ptc2-His_6 purification from an 11 gm frozen fermentation *Pichia* cell pellet is shown from total cell lysate to purified protein (Figure 14). The total amount of purified Ret/ptc2-His_6 is approximately 1.5-2.0 mg.

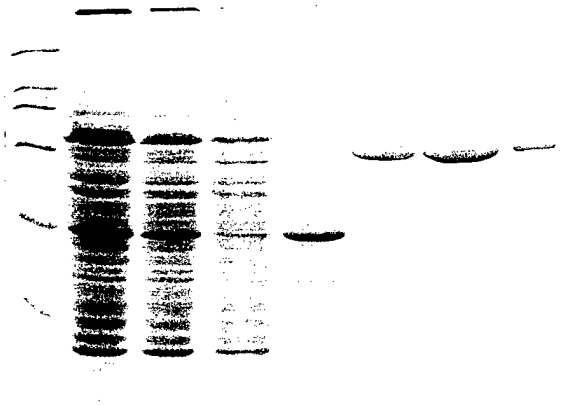

Figure 14. Western analysis of Ret/ptc2-His_6 with polyclonal Ret antibody. From left to right: BRL molecular weight markers, total cell lysate, supernatant fraction, dialyzed 55% NH_4SO_4 supernatant, pooled DE-52 fractions, pooled UnoQ6 fractions, concentrated UnoQ6 fractions, pooled gel filtration fractions.

II. Mitogenic Signaling of Ret/ptc2

Paxillin Co-Immunoprecipitates with Ret/ptc2

Western analysis of *ret/ptc2* transiently transfected HEK293 cells with polyclonal rabbit Ret antibodies shows Ret/ptc2 is expressed as a soluble protein (Figure 15A, upper panel). Immunoprecipitation of Ret/ptc2 from the supernatant fraction (S1) of HEK293 cells transiently transfected with *ret/ptc2* and Western analysis with monoclonal mouse paxillin antibodies reveals paxillin co-immunoprecipitates with Ret/ptc, whereas buffer transfected cells do not express Ret/ptc2 nor is paxillin immunopreciptitated (Figure 15A, lower panel). The four C-terminal LIM domains of paxillin was expressed as a GST-fusion protein and this substrate, GST-Pax_{LIM4}, is phosphorylated *in vitro* by HEK293 expressed Ret/ptc2, whereas the S1 fraction from buffer, 10 mM Tris-Cl, pH 8, 1 mM EDTA (TE, pH 8) transfected cells was unable to phosphorylate GST-Pax_{LIM4}, nor was the substrate capable of autophosphorylation (Figure 15B).

Phospho-Ret/ptc2 and Phospho-Paxillin Co-Immunoprecipitates with Phospho-p125^{FAK}

Western analysis with phosphotyrosine antibodies (PY-20) of Ret immunoprecipitated proteins reveals a prominant high molecular weight protein at approximately 125 kDa as well as tyrosyl-phosphorylated Ret/ptc2 and paxillin (Figure 15C).

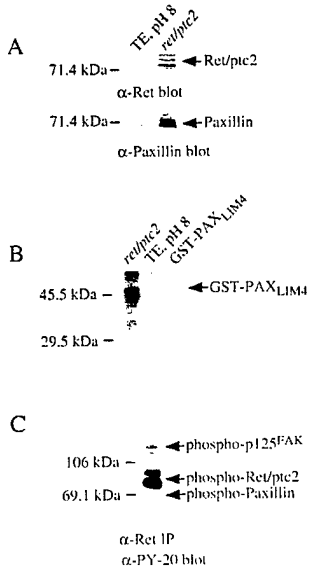

Figure 15. Ret/ptc2 is expressed in *ret/ptc2* transfected HEK293 cells (panel A, upper blot) and paxillin co-immunoprecipitates with Ret/ptc2 from *ret/ptc2* transfected cells (panel B, lower blot). Autoradiogram of GST-Pax_{LIM4} phosphorylated by Ret/ptc2 (panel B) *in vitro*. Paxillin, $p125^{FAK}$, and Ret/ptc2 co-immunoprecipitate and are tyrosyl-phosphorylated in *ret/ptc2* transfected HEK293 cells (panel C).

Western analyses with Ret antibodies (Figure16, upper panel) or PY-20 antibodies (Figure 16, lower panel) of polyclonal rabbit p125^{FAK} immunoprecipitated proteins from *ret/ptc2* transfected HEK293 cells show Ret/ptc2 (Figure 16, upper panel lanes 3, 6, 9 and 12) associates with p125^{FAK}, whereas Ret/ptc2 was not expressed or immunoprecipitated from either TE, pH 8 (Figure 16, upper panel lanes 1, 4, 7 and 10), nor vector, pRc/CMV (Figure 16, upper panel, lanes 2, 5, 8 and 11) transfected cells. Interestingly, only tyrosyl-phosphorylated Ret/ptc2 co-immunoprecipitated with tyrosyl-phosphorylated p125^{FAK} (Figure 16, lower panel, compare lanes 9 and 12). Similar studies in which Na_3VO_4 was not included in the preparation of the S1 fraction revealed a greater pool of unphosphorylated Ret/ptc2 which did not co-immunoprecipitate with p125^{FAK} (data not shown).

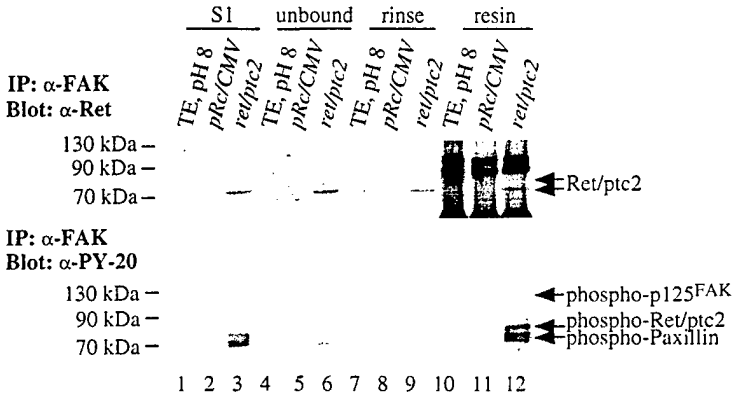

Figure 16. Polyclonal p125^{FAK} antibody co-immunoprecipitates tyrosyl-phosphorylated Ret/ptc2. Upper panel: Western analysis with Ret antibodies of p125^{FAK} immunoprecipitated proteins. Lower panel: Western analysis of p125^{FAK} immunoprecipitates using PY-20 antibodies.

Ret/ptc2 Activates c-Myc-ERK2 and not HA-JNK

Normalized values for the *in vitro* phosphorylation of myelin basic protein (MBP) by immunopreciptated c-*Myc*-ERK2 from *ret/ptc2* transfected HEK293 cells reveals ERK2 is activated in *ret/ptc2* transfected cells (Figure 17A). The level of ERK2 activity is similar in the presence or absence of serum. Western analysis of S1 fractions isolated from these transfected cells confirms the expression of Ret/ptc2 and p125^{FAK} Y397F (Figure 17B, upper and middle panels). Both Ret/ptc2 and p125^{FAK} are tyrosyl-phosphorylated (Figure 17B, lower panel). Increased ERK2 activity from *ret/ptc2-p125^{FAK}Y397F* co-transfected cells (Figure 17A) correlates with increased phospho-p125^{FAK}Y397F (Figure 17B, middle and lower panels). Ret/ptc2 does not activate the JNK pathway since *in vitro* phosphorylation of c-Jun by immunoprecipitated HA-JNK from cells co-transfected with *ret/ptc2-ha-jnk* was identical to that measured for vector controls (data not shown).

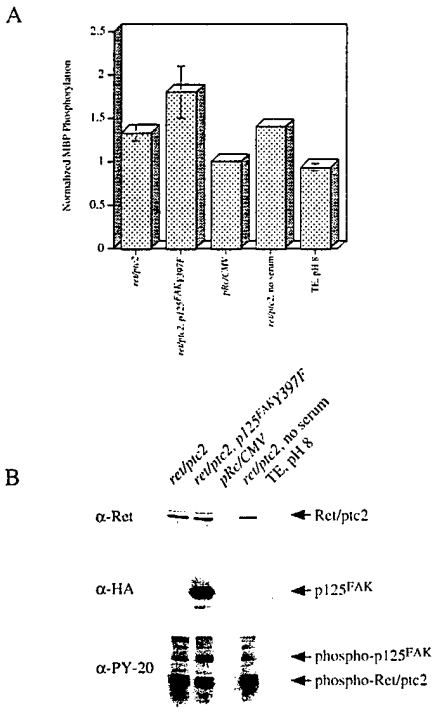

Figure 17. Co-transfected HEK293 cells express phospho-Ret/ptc2, phospho-p125^{FAK}Y397F, and activate c-*Myc*-ERK2. Panel A: Normalized values for the *in vitro* phosphorylation of myelin basic protein (MBP) by immunoprecipitated c-*Myc*-ERK2 isolated from transfected HEK293 cells. Panel B: Western analysis of HEK293 S1 fractions following co-transfection show *ret/ptc2* and *ret/ptc2-p125^{FAK}Y397F* express phospho-Ret/ptc2 (upper and lower blots). Phospho-Ret/ptc2 is expressed in the absence of serum (upper and lower blots). HA-tagged p125^{FAK}Y397F is expressed and tyrosyl-phosphorylated (middle and lower blots).

Ret/ptc2 and Ret/ptc2Y586F Activate the c-fos Promoter

Co-transfection of HEK293 cells with *ret/ptc2* and a c-*fos* promoter-luciferase reporter plasmid, p2FTL, shows the c-*fos* promoter is activated 12-fold above that measured from cells transfected with the pRc/CMV plasmid control (Figure 18). c-*fos* activity was increased 33% in cells co-transfected with *ret/ptc2-p125^{FAK}Y397F*. To determine whether Ret/ptc2 could activate the c-*fos* promoter independently of Shc, we employed the Shc independent Ret/ptc2 mutant, *ret/ptc2Y586F*. Our results show the c-*fos* promoter is activated 75% in cells transfected with *ret/ptc2Y586F*; activity is fully restored in cells co-transfected with *ret/ptc2Y586F-p125^{FAK}Y397F*. Interestingly, co-transfection of *ret/ptc2* or *ret/ptc2Y586F* with dominant negative Ras, *ras17N*, activated the c-*fos* promoter 25%; co-transfection with *p125^{FAK}Y396F* increased c-*fos* promoter activation to 33%. Co-transfection of cells with *ret/ptc2* and dominant negative Raf-1 abrogates c-*fos* activation which is not restored by the presence of p125^{FAK}Y397F. The Ret/ptc2 kinase domain (*ret/ptc2Δ1-235*) decreased c-*fos* activation below vector control levels which is suggestive of a dominant negative effect.

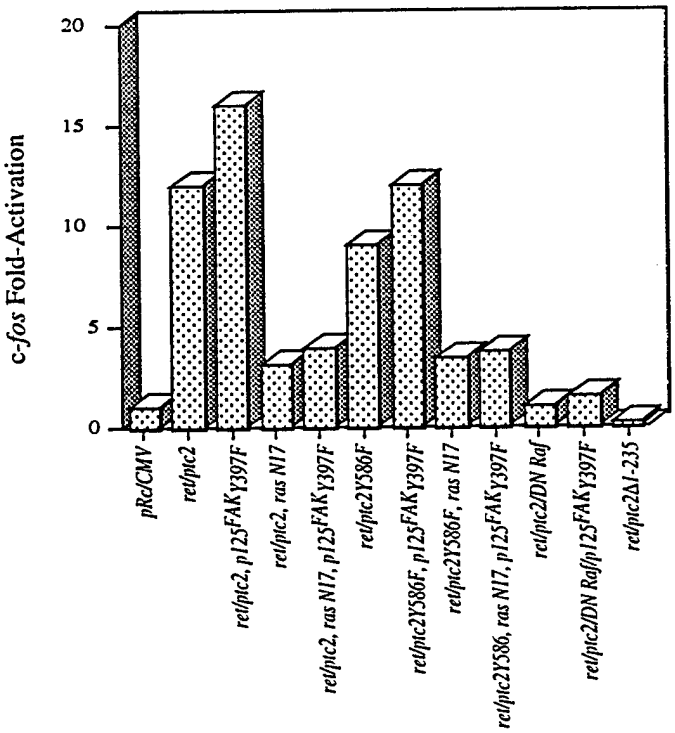

Figure 18. The c-*fos* promoter/luciferase reporter is activated 12-fold and 9-fold above vector transfected cells in *ret/ptc2* and *ret/ptc2Y586F* transfected HEK293 cells, respectively. The presence of p125^{FAK}Y397F increases c-*fos* promoter activity 33% in *ret/ptc2* and *ret/ptc2Y586F* co-transfected HEK293 cells. Dominant negative Ras, Ras17N, activates the c-*fos* promoter 25% when co-transfected with either *ret/ptc2* or *ret/ptc2Y586F*; the presence of p125^{FAK}Y586F increases c-*fos* activity 33%. Dominant negative Raf decreases c-*fos* promoter actvation to background levels.

Ret/ptc2 and Ret/ptc2Y586F Increase Cellular Tyrosine Phosphorylation in Microinjected NIH3T3 Cells

ret/ptc2 and *ret/ptc2Y586F* transfected HEK293 cells exhibit loss of cell-cell contact inhibition and isolated cells have a rounded, swollen morphology 16 hours post-transfection consistent with a transformed phenotype. Transfected cells exhibit numerous actin microspikes at their periphery 36 hours post-transfection while retaining their swollen phenotype, and adhesion to the plastic cell culture dishes is more stable 36 hours post-transfection than after 16 hours (data not shown).

Ret/ptc2, Ret/ptc2Y586F, and Ret/ptc2Δ1-235 accumulate in the cytosol of nuclear injected NIH3T3 cells (Figure19, panels a, b, d, e, g, h). Cells expressing Ret/ptc2 and Ret/ptc2Y586F exhibit an elongated phenotype (Figure 19, panels a, b, d, e) and cellular phosphotyrosine levels are increased (Figure 19, panels a-c, d-f), whereas cells expressing Ret/ptc2Δ1-235 do not exhibit these changes (Figure 19, panels g-i).

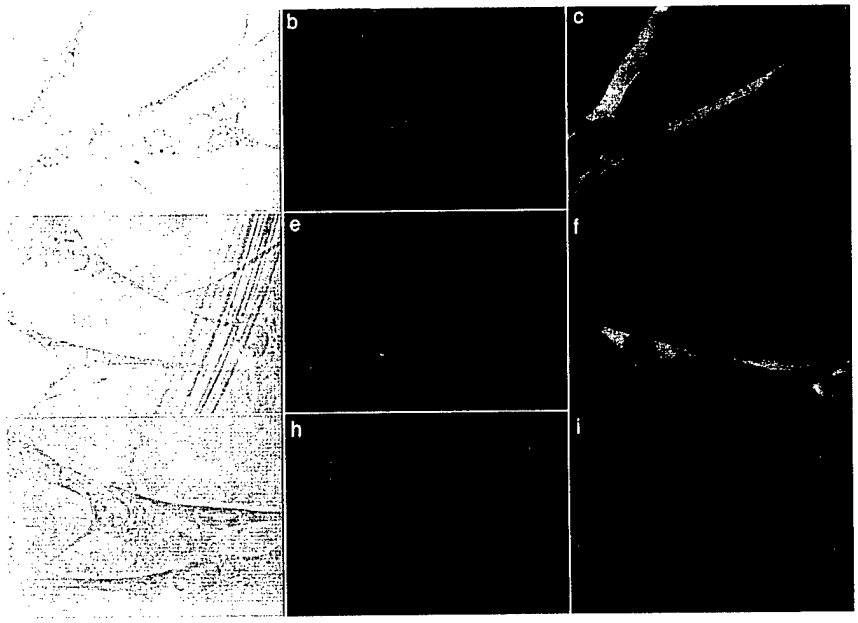

Figure 19. Expression of Ret/ptc2 and Ret/ptc2Y586F increases the level of cellular phosphotyrosine and cells exhibit an elongated phenotype in microinjected NIH3T3 cells. Cells expressing Ret/ptc2Δ1-235 do not exhibit these changes.

Ret/ptc2 and Ret/ptc2Y586F Phosphorylate p125^{FAK}Y397F

Western analysis using PY-20, Ret/ptc2 and 12CA5 antibodies of 12CA5 immunoprecipitated p125^{FAK}Y397F from transiently transfected HEK293 cells show p125^{FAK}Y397F (Figure 20A), Ret/ptc2, Ret/ptc2Y586F, and Ret/ptc2Δ1-235 are expressed (Figure 20B). The 12CA5 antibody appears to recognize Ret/ptc2 and Ret/ptc2Y586F because both proteins are detectable at longer exposure times of the 12CA5 Western blot (Figure 20A, lanes 2 and 5), whereas Ret/ptc2Δ1-235 is not detectable by the 12CA5 antibodies. p125^{FAK}Y397F, Ret/ptc2 and Ret/ptc2Y586F are tyrosyl-phosphorylated (Figure 20C). Although the amount of immunoprecipitated p125^{FAK}Y397F is equivalent in the co-transfected cells (Figure 20A, lanes 6-8), phosphorylation of p125^{FAK}Y397F is 50%

greater in *ret/ptc2* co-transfected cells than in *retptc2Y586F* co-transfected cells (Figure 20C, lanes 6 and 7). Ret/ptc2Δ1-235 is expressed (Figure 20B), however, Ret/ptc2Δ1-235 is not phosphorylated (compare Figure 20B and 20C, lanes 3 and 8), nor is immunoprecipitated p125^{FAK}Y397F phosphorylated (Figure 20C, lane 8). The differences in phosphotyrosine staining between Ret/ptc2, Ret/ptc2Y586F and Ret/ptc2Δ1-235 expressed in HEK293 cells reflect that observed in microinjected NIH3T3 cells (Figure 19).

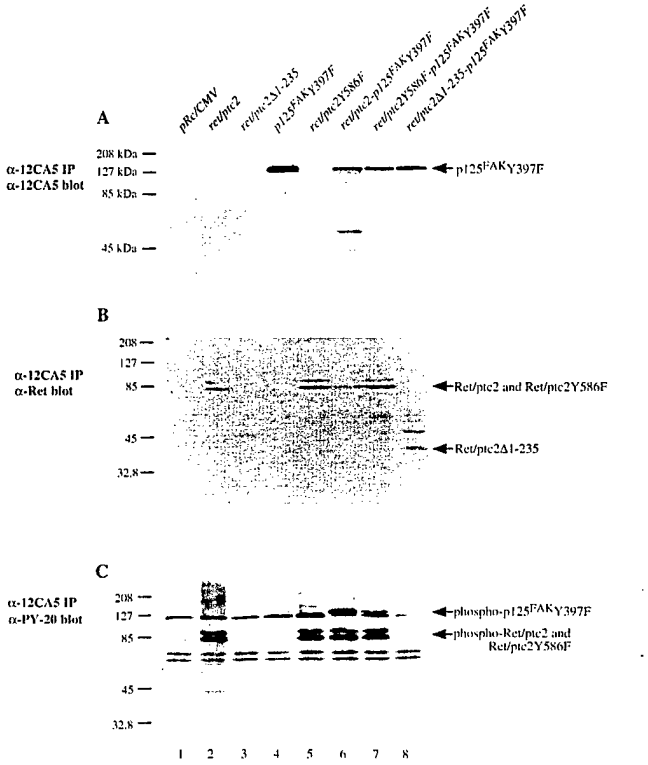

Figure 20. Transiently transfected HEK293 cells express p125^{FAK}Y397F (panel A), Ret/ptc2, Ret/ptc2Y586F, and Ret/ptc2Δ1-235 (panel B). p125^{FAK}Y397F is phosphorylated by phospho-Ret/ptc2 and phospho-Ret/ptc2Y586F, but not by unphosphorylated Ret/ptc2Δ1-235.

DISCUSSION

The *in vivo* association of Ret/ptc2 with paxillin and phosphorylation of the paxillin C-terminal LIM domains by Ret/ptc2 *in vitro* indicate paxillin is a suitable physiological substrate for Ret/ptc2. The association of Ret/ptc2 with paxillin is consistent with earlier reports of paxillin phosphorylation in Ret kinase signaling in NIH3T3 cells (53). The interaction of Ret/ptc2 with paxillin and p125^{FAK} is likely to be mediated by the Ret tyrosine kinase domain since paxillin co-immunoprecipitates, albeit to a weaker extent, with

Ret/ptc2Δ1-235 (data not shown), and Ret/ptc2Δ1-235 co-immunprecipitates with p125^{FAK}Y397F. Ret/ptc2Δ1-235 is not catalytically active (V. Yao, unpublished data), does not phosphorylate p125^{FAK} Y397F, and appears to inhibit activation of the c-*fos* promoter. The association of Ret/ptc2 with p125^{FAK} and paxillin is not surprising since p125^{FAK} binds directly to paxillin (51). The phosphorylation of p125^{FAK}, however, implicates activation of the Ras signaling pathway (54).

Our results show the increased activity of c-*myc*-ERK2 from *ret/ptc2* transfected cells is not dependent on integrin receptor activation (55,56) since the absence of serum in the transfection medium does not abrogate the increased activity of immunoprecipitated ERK2 or the phosphorylation of p125^{FAK}. ERK2 activation of *ret/ptc2* transfected HEK293 cells is concommitant with c-*fos* activation. Increased ERK2 and c-*fos* activity in *ret/ptc2-p125^{FAK}Y397F* co-transfectants indicate p125^{FAK}Y397F increases Ras pathway signaling possibly by functioning as an exogenous substrate source. Since c-Src binding to p125^{FAK} at Y397 is necessary for p125^{FAK} phosphorylation at Y925 followed by Grb2 recruitment (57-59), our results with the p125^{FAK}Y397F mutant show constitutively active Ret/ptc2 effectively circumvents c-Src regulation of p125^{FAK}.

Although Ras activation had been demonstrated for Ret/ptc2 signaling by association with Shc (38), we wanted to determine whether activation of the Ras pathway by Ret/ptc2 phosphorylation of p125^{FAK} could occur independently of Shc. Our results show that although the Ret/ptc2 Shc independent mutant, Ret/ptc2Y586F, is less catalytically active than Ret/ptc2, c-*fos* activation in *ret/ptc2Y586F- p125^{FAK}Y397F* co-transfectants is fully restored to levels measured from HEK293 cells transfected with *ret/ptc2* alone. These results indicate Ret/ptc2Y586F bypasses the c-Src regulation of p125^{FAK}Y397F. Activation of the Ras signaling pathway by Ret/ptc2Y586F phosphorylation of p125^{FAK} is independent of Shc recruitment. The decreased level of c-*fos* promoter activation by Ret/ptc2Y586F suggests the physiological activation of the Ras signaling cascade by Ret/ptc2 *in vivo* presumably consists of the additive interactions of both Shc recruitment and p125^{FAK} phosphorylation. The Ret/ptc2Y586F mutant was previously shown in microinjection studies to abolish DNA synthesis in 10 T1/2 cells, four hours post-injection (31). We show here that this mutant is capable of activating an early gene transcription factor in HEK293 cells harvested 36-48 hours post-transfection.

Surprisingly, co-transfection of dominant negative Ras, *ras17N* (60), with *ret/ptc2* or *ret/ptc2Y586F* does not abolish c-*fos* activation, thereby suggesting that Ret/ptc2 may activate other signal transduction cascades which result in early gene transcription. These results are consistent with earlier reports in which the interaction of PLCγ with residue Y539 (36,41) may be signaling via protein kinase C (61). The consistent increase of c-*fos*

activation from *ret/ptc2-ras17N* and *ret/ptc2Y586-ras17N* co-transfectants in the presence of *p125^{FAK}Y397* suggests phospho-p125^{FAK} elicits additional signaling pathways. One plausible candidate is the PI3 kinase pathway which has been reported to be involved in glial-derived neurotrophic factor stimulation of RetR (62). Phospho-p125^{FAK} has been implicated to activate other small GTPases such as Rac and Cdc42 via PI3 kinase (63) which induce actin polymerization and DNA synthesis independently of JNK/SAPK Map kinase pathway activation (64). Our studies support activation of Rac and Cdc42 since we observe the appearance of actin microspikes at the cell peripheries of *ret/ptc2* transfected HEK293 in the absence of JNK pathway activation. The unregulated induction of Rac or Cdc42 by phospho-p125^{FAK}-activated PI3 kinase in *ret/ptc2* transfected cells may provide a molecular basis for initiating cell motility in papillary thyroid carcinoma metastases.

Although c-*fos* activation is not abolished by Ras17N, co-transfection of HEK293 cells with dominant negative Raf inhibits c-*fos* activation. The contribution of c-*fos* activation via Raf constitutes 25% of full activation which is unlike the 75-90% reduction of Ret/ptc2 oncogenic activity observed upon mutation of the Ret/ptc2 PLCγ binding site at residue Y539 (41). Our results indicate a component of Ret/ptc2 activation of the Ras signaling pathway occurs at the level of Raf. Involvement of PKC in Ret/ptc2 signaling is a likely candidate as discussed above especially since direct activation of Raf has been demonstrated for PKC isoforms α and ε (65).

One perplexing aspect of Ret/ptc2 signaling concerns how is Ret/ptc2 recruited to the membrane to interact with membrane associated proteins such as Ras. The strong association and phosphorylation of the paxillin/p125^{FAK} complex by Ret/ptc2 could presumably lead to its membrane localization by either the 159 amino acid focal adhesion targeting sequence within the p125^{FAK} C-terminal tail (66), and/or the association of phospho-paxillin with another focal adhesion protein, vinculin (67,68). Alternatively, the association of the RIα dimerization domain with A-kinase anchoring proteins (AKAPs) (46,69) may provide another mechanism for Ret/ptc2 membrane localization. Western analysis using dual-specificity AKAP-1 antibodies (46) of Ret/ptc2 immunoprecipitated proteins from *ret/ptc2* transfected HEK293 cells identified a high molecular weight band (data not shown) characteristic of AKAPs (46,69,70). It is yet unclear whether the RIα dimerization domain is necessary for Ret/ptc2 catalytic activity or association with AKAPs. Our previous studies have shown the cAPK RIα dimerization domain in Ret/ptc2 is absolutely required for eliciting a mitogenic response (31). In addition, the association of Ret/ptc2 with Enigma has been shown to provide another means for membrane localization (38).

We propose active Ret/ptc2 is inappropriately localized to the membrane by its association with the paxillin/p125^{FAK} complex and/or by association of the RIα dimerization domain to an AKAP isoform. Unregulated phosphorylation of paxillin and p125^{FAK} by Ret/ptc2 enhances signaling of the Ras pathway independently of Shc and bypasses c-Src regulation of p125^{FAK} phosphorylation. Ret/ptc2 activation of the c-*fos* promoter is decreased 25% in the presence of Ras17N and decreases to background levels in the presence of dominant negative Raf. Ret/ptc2 presumably activates Raf by PLCγ-mediated activation of PKC and indirectly activates GTPases such as Rac and Cdc42 via p125^{FAK} phosphorylation (Figure 21). The physiological consequences of improper localization and unregulated phosphorylation of local proteins by Ret/ptc2 leads to an inordinate activation of the mitogenic Ras signaling pathway mediated by increased ERK2 activity. Our results show Ret/ptc2 adroitly utilizes a variety of diverse cellular signaling components to effect cellular transformation and proliferation as well as the capablity for manipulating focal adhesion protein signaling pathways which have been linked to initiating cell motility.

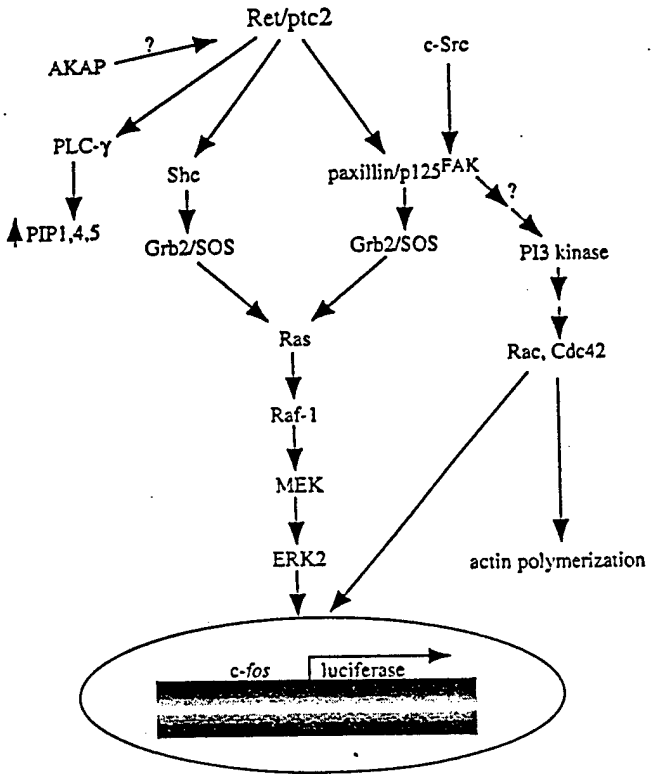

Figure 21. Model of Ret/ptc2 signaling.

CONCLUSIONS

We have modeled the kinase portion of RetR based on our structure of the cAPK C-subunit and on the crystal structure of the insulin receptor kinase domain. This has provided a structural framework for the rest of our research. We are now focusing on a comprehensive model of all of the genetic lesions and are looking closely at the C-terminal tail for similarities to the catalytic subunit of cAPK.

With the microinjection assay we have been able to establish what is essential for the mitogenic properties of *ret/ptc2*. In conjunction with this, we have used the yeast two-hybrid system to identify Ret/ptc2 binding proteins. The surprising discovery that Enigma binds specifically to Ret/ptc2 has introduced a potentially important and novel element to this signaling pathway. We have found Ret/ptc2 and Enigma co-distributes in microinjected fibroblasts using confocal microscopy.

We have used a unique approach of employing chimeric forms of Ret/ptc2, Enigma and Shc to test whether Enigma localization or Shc interaction is important for Ret/ptc2 mitogenic signaling. Mutants of Ret/ptc2 in which the Shc docking site was absent were unable to phosphorylate Shc and were mitogenically inactive. A deletion mutant of Ret/ptc2 that lacked an Enigma docking site was diffusely spread throughout the cytoplasm and also lacked mitogenic activity. When the Enigma docking site of Ret/ptc2 was replaced with the PDZ domain of Enigma, Ret/ptc2 was once again targeted to the cell edges, but this chimeric protein was unable to bind Shc and was mitogenically inactive. Mitogenic activity was restored only when this properly targeted form of Ret/ptc2 was co-expressed with the chimeric form of Shc, PLCγShc, a protein that is capable for interaction. These results indicate that both sub-cellular targeting of Ret/ptc2 by Enigma and interaction with phosphorylated Shc are required for Ret/ptc2 mitogenic signaling.

We have also identified several A-kinase anchoring proteins from our yeast two-hybrid screen that bind to the N-terminus of RIα. These proteins have now been cloned and expressed in *E. coli*. Like Enigma, the physiological role of this novel family of proteins is still not clear. If docking of Ret/ptc2 to specific subcellular sites are important, then we shall also mutate residues within the dimerization domain of RIα to see if we can isolate mutant forms of Ret/ptc2 that are still dimers but no longer mitogenic.

In parallel with the microinjection studies we have developed a mammalian expression system in transiently transfected HEK293 cells and a yeast expression system that yields mg quantities of Ret/ptc2. We have used Ret/ptc2 expressed in mammalian cells to evaluate peptide substrates and to develop an *in vitro* kinase assay. The overexpression and purification of active, phosphorylated Ret/ptc2-His_6 in the yeast, *Pichia pastoris*, has

allowed us to pursue a vigorous and comprehensive biochemical and biophysical analyses of this unique oncogene at the molecular level. The results obtained so far are promising.

Expression of Ret/ptc2 in HEK293 cells have enabled us to link the contributions of various SH2 domain proteins identified in our earlier yeast two-hybrid screen to construct a comprehensive model for Ret/ptc2 signaling. The activation of focal adhesion kinase by the Ret/ptc2 oncogene provides a biochemical basis for promoting cell motility which is the fundamental step for metastases of carcinomas.

REFERENCES

1. Hanks, S. K., and Hunter, T. (1995) *Faseb J* **9**(8), 576-96
2. Taylor, S. S., Buechler, J. A., and Yonemoto, W. (1990) *Annu Rev Biochem* **59**(971), 971-1005
3. Knighton, D. R., Zheng, J. H., Ten, E. L., Ashford, V. A., Xuong, N. H., Taylor, S. S., and Sowadski, J. M. (1991) *Science* **253**(5018), 407-14
4. Taylor, S. S., Knighton, D. R., Zheng, J., Ten, E. L., and Sowadski, J. M. (1992) *Annu Rev Cell Biol* **8**(429), 429-62
5. Takahashi, M., Buma, Y., and Taniguchi, M. (1991) *Oncogene* **6**(2), 297-301
6. Pachnis, V., Mankoo, B., and Costantini, F. (1993) *Development* **119**(4), 1005-17
7. Schuchardt, A., D'Agati, V., Larsson, B. L., Costantini, F., and Pachnis, V. (1994) *Nature* **367**(6461), 380-3
8. Sugaya, R., Ishimaru, S., Hosoya, T., Saigo, K., and Emori, Y. (1994) *Mech Dev* **45**(2), 139-45
9. Trupp, M., Arenas, E., Fainzilber, M., Nilsson, A. S., Sieber, B. A., Grigoriou, M., Kilkenny, C., Salazar, G. E., Pachnis, V., Arumae, U., and et, a. l. (1996) *Nature* **381**(6585), 785-8
10. Jing, S., Wen, D., Yu, Y., Holst, P. L., Luo, Y., Fang, M., Tamir, R., Antonio, L., Hu, Z., Cupples, R., Louis, J. C., Hu, S., Altrock, B. W., and Fox, G. M. (1996) *Cell* **85**(7), 1113-24
11. Treanor, J. J., Goodman, L., de, S. F., Stone, D. M., Poulsen, K. T., Beck, C. D., Gray, C., Armanini, M. P., Pollock, R. A., Hefti, F., Phillips, H. S., Goddard, A., Moore, M. W., Buj, B. A., Davies, A. M., Asai, N., Takahashi, M., Vandlen, R., Henderson, C. E., and Rosenthal, A. (1996) *Nature* **382**(6586), 80-3

12. Durbec, P., Marcos, G. C., Kilkenny, C., Grigoriou, M., Wartiowaara, K., Suvanto, P., Smith, D., Ponder, B., Costantini, F., Saarma, M., and et, a. l. (1996) *Nature* **381**(6585), 789-93
13. Sanchez, M. P., Silos, S. I., Frisen, J., He, B., Lira, S. A., and Barbacid, M. (1996) *Nature* **382**(6586), 70-3
14. Takahashi, M., Ritz, J., and Cooper, G. M. (1985) *Cell* **42**(2), 581-8
15. Ishizaka, Y., Tahira, T., Ochiai, M., Ikeda, I., Sugimura, T., and Nagao, M. (1988) *Oncogene Res* **3**(2), 193-7
16. Kunieda, T., Matsui, M., Nomura, N., and Ishizaki, R. (1991) *Gene* **107**(2), 323-8
17. Mulligan, L. M., Eng, C., Healey, C. S., Clayton, D., Kwok, J. B., Gardner, E., Ponder, M. A., Frilling, A., Jackson, C. E., Lehnert, H., and et, a. l. (1994) *Nat Genet* **6**(1), 70-4
18. Hofstra, R. M., Landsvater, R. M., Ceccherini, I., Stulp, R. P., Stelwagen, T., Luo, Y., Pasini, B., Hoppener, J. W., van, A. H., Romeo, G., and et, a. l. (1994) *Nature* **367**(6461), 375-6
19. Edery, P., Lyonnet, S., Mulligan, L. M., Pelet, A., Dow, E., Abel, L., Holder, S., Nihoul, F. C., Ponder, B. A., and Munnich, A. (1994) *Nature* **367**(6461), 378-80
20. Romeo, G., Ronchetto, P., Luo, Y., Barone, V., Seri, M., Ceccherini, I., Pasini, B., Bocciardi, R., Lerone, M., Kaariainen, H., and et, a. l. (1994) *Nature* **367**(6461), 377-8
21. Grieco, M., Santoro, M., Berlingieri, M. T., Melillo, R. M., Donghi, R., Bongarzone, I., Pierotti, M. A., Della, P. G., Fusco, A., and Vecchio, G. (1990) *Cell* **60**(4), 557-63
22. Grieco, M., Cerrato, A., Santoro, M., Fusco, A., Melillo, R. M., and Vecchio, G. (1994) *Oncogene* **9**(9), 2531-5
23. Bongarzone, I., Monzini, N., Borrello, M. G., Carcano, C., Ferraresi, G., Arighi, E., Mondellini, P., Della, P. G., and Pierotti, M. A. (1993) *Mol Cell Biol* **13**(1), 358-66
24. Bongarzone, I., Butti, M. G., Coronelli, S., Borrello, M. G., Santoro, M., Mondellini, P., Pilotti, S., Fusco, A., Della, P. G., and Pierotti, M. A. (1994) *Cancer Res* **54**(11), 2979-85
25. Tong, Q., Li, Y., Smanik, P. A., Fithian, L. J., Xing, S., Mazzaferri, E. L., and Jhiang, S. M. (1995) *Oncogene* **10**(9), 1781-1787
26. Minoletti, F., Butti, M. G., Coronelli, S., Miozzo, M., Sozzi, G., Pilotti, S., Tunnacliffe, A., Pierotti, M. A., and Bongarzone, I. (1994) *Genes, Chromsomes & Cancer* **11**, 51-57

27. Santoro, M., Dathan, N. A., Berlingieri, M. T., Bongarzone, I., Paulin, C., Grieco, M., Pierotti, M. A., Vecchio, G., and Fusco, A. (1994) *Oncogene* **9**(2), 509-16
28. Bubis, J., Vedvick, T. S., and Taylor, S. S. (1987) *J Biol Chem* **262**(31), 14961-6
29. Leon, D. A., Dostmann, W. R. G., and Taylor, S. S. (1991) *Biochemistry* **30**(12), 3035-40
30. Su, Y., Dostmann, W. R. G., Herberg, F. W., Durick, K., Xuong, N.-h., Ten Eyck, L., Taylor, S. S., and Varughese, K. I. (1995) *Science* **269**, 807-813
31. Durick, K., Yao, V. J., Borrello, M. G., Bongarzone, I., Pierotti, M. A., and Taylor, S. S. (1995) *J Biol Chem* **270**(42), 24642-5
32. Vojtek, A. B., Hollenberg, S. M., and Cooper, J. A. (1993) *Cell* **74**(1), 205-14
33. Santoro, M., Wong, W. T., Aroca, P., Santos, E., Matoskova, B., Grieco, M., Fusco, A., and di, F. P. (1994) *Mol Cell Biol* **14**(1), 663-75
34. Pandey, A., Duan, H., Di, F. P., and Dixit, V. M. (1995) *J Biol Chem* **270**(37), 21461-3
35. Wu, R. Y., and Gill, G. N. (1994) *J Biol Chem* **269**(40), 25085-90
36. Durick, K., Wu, R. Y., Gill, G. N., and Taylor, S. S. (1996) *J Biol Chem* **271**(22), 12691-4
37. Wu, R., Durick, K., Songyang, Z., Cantley, L. C., Taylor, S. S., and Gill, G. N. (1996) *J Biol Chem* **271**(27), 15934-41
38. Durick, K., Gill, G. N., and Taylor, S. S. (1998) *Mol Cell Biol* **18**(4), 2298-308
39. Lorenzo, M. J., Gish, G. D., Houghton, C., Stonehouse, T. J., Pawson, T., Ponder, B. A., and Smith, D. P. (1997) *Oncogene* **14**(7), 763-71
40. Arighi, E., Alberti, L., Torriti, F., Ghizzoni, S., Rizzetti, M. G., Pelicci, G., Pasini, B., Bongarzone, I., Piutti, C., Pierotti, M. A., and Borrello, M. G. (1997) *Oncogene* **14**(7), 773-82
41. Borrello, M. G., Alberti, L., Arighi, E., Bongarzone, I., Battistini, C., Bardelli, A., Pasini, B., Piutti, C., Rizzetti, M. G., Mondellini, P., Radice, M. T., and Pierotti, M. A. (1996) *Mol Cell Biol* **16**(5), 2151-63
42. Takahashi, M., Buma, Y., and Hiai, H. (1989) *Oncogene* **4**(6), 805-6
43. Liu, X., Vega, Q. C., Decker, R. A., Pandey, A., Worby, C. A., and Dixon, J. E. (1996) *J Biol Chem* **271**(10), 5309-12
44. Hubbard, S. R., Wei, L., Ellis, L., and Hendrickson, W. A. (1994) *Nature* **372**, 746-754
45. Songyang, Z., Carraway, K. L., Eck, M. J., Harrison, S. C., Feldman, R. A., Mohammadi, M., Schlesslinger, J., Hubbard, S. R., Smith, D. P., Eng, C.,

Lorenzo, M. J., Ponder, B. A. J., Mayer, B. J., and Cantley, L. C. (1995) *Nature* **373**(6514), 536-539

46. Huang, L.-S., Durick, K., Weiner, J., Chun, J., and Taylor, S. (1997) *PNAS* **94,** 11184-11189
47. Gleeson, M. A. G., White, C. E., Meininger, D. P., and Komives, E. A. (1998) *Generation of Protease Deficient Strains of Pichia pastoris and Their Use in Heterologous Protein Expression* in Methods in Molecular Biology (Higgins, D.R. and Cregg, J.M., Eds.), **103,** pp.81-94, Humana Press, Totowa, NJ
48. Sambrook, J., Fritsch, E. F., and Maniatis, T. (1989) *Molecular Cloning: A Laboratory Manual*, 2nd Ed. Ed. (Nolan, C., Ferguson, M., and Ford, N., Eds.), Cold Spring Harbor Laboratory Press, Cold Spring Harbor, NY
49. Laemmli, U. K. (1970) *Nature* **227**(259), 680-5
50. Doolittle, R. F. (1986) *Of urfs and orfs: A primer on how to analyze derived amino acid sequences*, University Science Books, Mill Valley, CA
51. Turner, C. E., and Miller, J. T. (1994) *J Cell Sci* **107**(Pt 6), 1583-91
52. Li, Y. S., Shyy, J. Y., Li, S., Lee, J., Su, B., Karin, M., and Chien, S. (1996) *Mol Cell Biol* **16**(11), 5947-54
53. Romano, A., Wong, W. T., Santoro, M., Wirth, P. J., Thorgeirsson, S. S., and Di Fiore, P. P. (1994) *Oncogene* **9**(10), 2923-33
54. Schlaepfer, D. D., and Hunter, T. (1996) *Mol Cell Biol* **16**(10), 5623-33
55. Guan, J. L., Trevithick, J. E., and Hynes, R. O. (1991) *Cell Regul* **2**(11), 951-64
56. Kornberg, L. J., Earp, H. S., Turner, C. E., Prockop, C., and Juliano, R. L. (1991) *Proc Natl Acad Sci U S A* **88**(19), 8392-6
57. Guan, J. L., and Shalloway, D. (1992) *Nature* **358**(6388), 690-2
58. Hanks, S. K., and Polte, T. R. (1997) *Bioessays* **19**(2), 137-45
59. Schlaepfer, D. D., Hanks, S. K., Hunter, T., van, der, Geer, and P. (1994) *Nature* **372**(6508), 786-91
60. Cai, H., Szeberenyi, J., and Cooper, G. M. (1990) *Mol Cell Biol* **10**(10), 5314-23
61. Santoro, M., Melillo, R. M., Grieco, M., Berlingieri, M. T., Vecchio, G., and Fusco, A. (1993) *Cell Growth Differ* **4**(2), 77-84
62. van Weering, D., and Bos, J. (1997) *j cell biol* **272**(1), 249-254
63. Symons, M. (1996) *Trends Biochem Sci* **21**(5), 178-81
64. Lamarche, N., Tapon, N., Stowers, L., Burbelo, P. D., Aspenstrom, P., Bridges, T., Chant, J., and Hall, A. (1996) *Cell* **87**(3), 519-29
65. Cai, H., Smola, U., Wixler, V., Eisenmann, T. I., Diaz, M. M., Moscat, J., Rapp, U., and Cooper, G. M. (1997) *Mol Cell Biol* **17**(2), 732-41

66. Hildebrand, J. D., Schaller, M. D., and Parsons, J. T. (1993) *J Cell Biol* **123**(4), 993-1005
67. Brown, M. C., Perrotta, J. A., and Turner, C. E. (1996) *J Cell Biol* **135**(4), 1109-23
68. Turner, C. E., Glenney, J., Jr., and Burridge, K. (1990) *J Cell Biol* **111**(3), 1059-68
69. Li, Y., Ndubuka, C., and Rubin, C. S. (1996) *J Biol Chem* **271**(28), 16862-9
70. Dell'Acqua, M. L., and Scott, J. D. (1997) *J Biol Chem* **272**(20), 12881-4

BIBLIOGRAPHY AND PERSONNEL

PUBLICATIONS

1. Durick, K., Yao, V.J., Borrello, M.G., Bongarzone, I., Pierotti, M.A., and Taylor, S.S. Tyrosines outside the kinase core and dimerization are required for the mitogenic activity of RET/ptc2. *J. Biol. Chem.* **270**, 2464224645 (1995).

2. Durick, K., Wu, R-Y., Gill, G., and Taylor, S.S. Mitogenic signaling by Ret/ptc2 Requires Association with Enigma via a LIM Domain. *J. Biol. Chem.* **271**, 12691-12694 (1996).

3. Wu, R-Y., Durick, K., Songyang, Z., Cantley. L., and Taylor, S.S. Specificity of LIM Domain Interactions with Receptor Tyrosine Kinases. *J. Biol. Chem.* **271**, 15934-15941 (1996).

4. Pandey, A., Durick, K.P., Liu, X., Vega, Q.C., Worby, C.A., Shen, S-H., Taylor, S.S., and Dixon, J.E. Identification of the SH2 containing phosphatase, PTP1C, as a target for the Ret receptor protein-tyrosine kinase. Submitted *Journal of Biological Chemistry.*

5. Yao, V.J., Mullins, R.D., Purcell, T. , and Taylor, S.S. Expression, Purification, and Biophysical Characterization of the Human Oncogene, Ret/ptc2. *UC San Diego, Dept. of Chemistry & Biochemistry, La Jolla, CA 92093-0654, #Structure Biology Laboratory, The Salk Institute, La Jolla, CA 92037, @Invitrogen Corporatioon, Carlsbad, CA 92008. Beckman Symposium on Solution Interactions of Macromolecules, November 14-17, 1997, Galveston, TX, Poster Presentation.

6. Yao, V.J., Guy, P.M., Shyy, J. Y.-J., and Taylor, S.S. Activation of the Mitogenic Ras Signaling Pathway via Focal Adhesion Proteins by the Ret/ptc2 Oncogene. Department of Chemistry & Biochemistry, Department of Medicine, Department of Bioengineering, UC San Diego, La Jolla, CA 92093. Tyrosine Phosphorylation and Cell Signaling, August 15-19, 1998, The Salk Institute, La Jolla, CA, Poster Presentation.

7. Yao, V.J., Guy, P.M., Zimmerman, M.J., Shyy, J.Y.-J., Feramisco, J.R., and Taylor, S.S. Ret/ptc2 Enchances Ras Signaling by $p125^{FAK}$ Phosphorylation. (in preparation).

8. Yao, V.J., Komives, E. A., Mullins, R.D., Purcell, T., Pierotti, M.A., and Taylor, S.S. Expression and Characterization of the Human Oncoprotein, Ret/ptc2. (in preparation).

9. Yao, V.J. and Taylor, S.S. Kinetic Analysis of Ret/ptc2. (in preparation).

PERSONNEL

Durick, Kyle
Huttenmaier, Carolyn
Radzio-Andzelm, Elzbieta
Russell, Kristine
Taylor, Susan S.
Whitney, Michael
Yao, Virginia J.